The Tau Neutrino

Candidacy Paper

Ian T. Lawson
Department of Physics and Astronomy
University of Victoria
October 3, 1996

Abstract

The tau neutrino is a neutral third generation lepton contained within the Standard Model Family. Several experiments have been studying the properties of the tau neutrino, nevertheless it has yet to be directly observed. Several different methods that can allow one to study the mass of the tau neutrino are presented in this review. The measurements of the lifetime and magnetic moment of the tau neutrino are discussed and the relationship of the tau neutrino to astrophysical phenomena is presented.

Contents

1. Introduction

Approximately 75 years ago physicists were trying to explain the observation of a continuous energy spectrum of electrons emitted in nuclear beta-decays. W. Pauli suggested that perhaps a new particle, the neutrino, could be used to explain the beta-decay process.[1] Pauli postulated that this new particle would be neutral, weakly interacting and massless. In 1953 the electron neutrino (ν_e) was observed.[2] Later a second type of neutrino, the muon neutrino (ν_μ), was observed[3] and a third neutrino, the tau neutrino (ν_τ), is also expected to exist, but has yet to be observed directly.

Neutrinos are spin 1/2 particles that interact only through the weak force. Neutrinos have a zero electric charge. There is no evidence that the neutrinos have a mass, however, if they do have mass then there are several consequences. For example, massive neutrinos would likely be unstable[4]; and it may be possible for mixing to occur between the different types of neutrinos which would allow a neutrino to oscillate between one type and another (*eg.* $\nu_e \longleftrightarrow \nu_\mu$). Consequently the study of neutrino mass is of great physical interest.

An observation of a massive neutrino would have important implications to the fields of particle physics, astrophysics and cosmology.[4] In particle physics, massive neutrinos would provide a large window to physics beyond the Standard Model. Neutrino oscillations could explain the solar neutrino problem, where the observed number of neutrinos emitted from the sun is significantly less than the theoretically expected amount. In astrophysics, massive neutrinos would be candidates for the dark or missing matter component of the universe.

Experiments studying the properties of neutrinos can be divided into two categories. The first type of experiment does not detect the neutrino, instead it measures the other particles in a decay or reaction and infers the neutrino properties. The limits on the mass of the different types of neutrinos comes from such experiments, which will be described in the next section. The second type of experiment directly observes the neutrino in the detector. These experiments are difficult as the neutrino interacts only through the weak interaction. For example, only one neutrino in 10^{10} passing through the center of the earth is likely to interact. The experiments that discovered the electron and muon neutrino fall into this second category.

This paper reviews the measurements made to determine the mass of the third type of neutrino, called the tau neutrino. The remainder of this section will discuss

the theoretical and experimental properties of the tau neutrino and give its relation to the Standard Model. Section 2 reviews measurements of the tau neutrino mass from various tau decays. Section 3 reviews measurements of the tau neutrino mass from the Standard Model as well as astrophysical and cosmological properties. Section 4 discusses the consequences of a massive tau neutrino and Section 5 discusses future experiments and concludes this review.

1.1. Neutrino Properties

Of the three neutrinos only the ν_e and ν_μ have been directly observed by experiment. The ν_e was observed by Reines and Cowan *et. al.*[2] at the Hanford nuclear reactor in 1953 through antineutrino capture ($\overline{\nu}_e p \rightarrow e^+ n$). Nuclear fission in the reactor produced neutron-rich nuclides which subsequently beta-decayed creating large quantities of antineutrinos. Some of the antineutrinos from the reactor entered the detector filled with a water-cadmium mixture and occasionally an antineutrino would interact with a proton in a water molecule. The reaction ($\overline{\nu}_e p \rightarrow e^+ n$) created a positron that quickly annihilated into a photon pair that was detected in the liquid scintillation detectors surrounding the water container. The neutron drifted through the water-cadmium mixture until it was absorbed by the cadmium. The cadmium then released photons that were also detected in the scintillator. If the detection of these photons occurred between 0.75 and 30 μs after the detection of the photons from the positron, then this event was considered as a candidate for an electron antineutrino event. A diagram of the process used by Reines and Cowan at Hanford is shown in Figure 1.

The ν_μ was observed in 1962 by Lederman *et. al.*[3] at the Brookhaven National Accelerator Laboratory. A 15 GeV proton beam was directed onto a beryllium target creating a beam of 3 GeV pions and kaons (see Figure 2). The pions (kaons) decayed-in-flight into a muon and a muon antineutrino ($\pi^- \rightarrow \mu^- \overline{\nu}_\mu$ or $K^- \rightarrow \mu^- \overline{\nu}_\mu$). Because the pion (kaon) was highly relativistic, the decay products were collimated along the pion (kaon) direction. A 13.5 m iron shield placed in front of the detector removed all the charged particles from the antineutrino beam. The antineutrino beam then passed through a detector consisting of spark chambers sandwiched between aluminum plates. During the operation of the experiment, approximately 10^{16} protons collided into the beryllium target creating 10^{14} antineutrinos incident on the detector. A small number of antineutrinos interacted with the protons in the aluminum plates creating a muon and a neutron ($\overline{\nu}_\mu p \rightarrow \mu^+ n$). The muon was detected in the spark chambers while the neutron was not observed. In 1962, Lederman *et. al.* recorded a total of 29 events that were identified as muon antineutrinos.

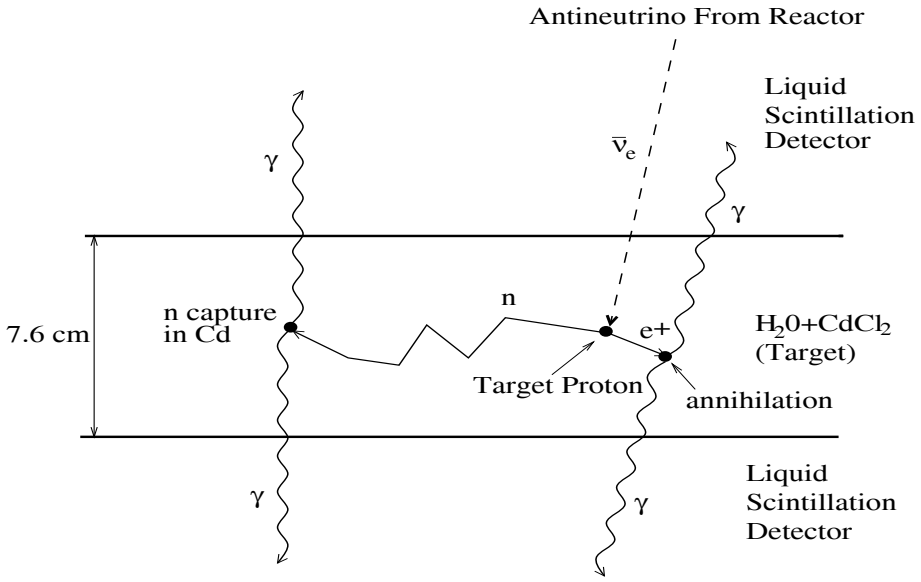

Figure 1: Schematic diagram of the electron antineutrino experiment performed by Reines and Cowan at the Hanford nuclear reactor. The experiment consisted of two tanks filled with water and cadmium-chloride with each tank sandwiched between 2 liquid scintillation detectors.

The third type of neutrino, the ν_τ, has not been directly observed because it is difficult to create a tau neutrino beam with sufficient intensity. In order to create a ν_τ beam, a particle that decays to a τ^- and a ν_τ would need to be produced. The tau lepton is much more massive than either the pion or kaon, therefore heavier particles, such as b-quark mesons would have to be used. A new accelerator, the LHC, is currently being constructed at CERN, that will have sufficient energy (14 TeV) to create a ν_τ beam.[5]

Currently there is no evidence that neutrinos have mass. The best experimental mass limit for the ν_e, 5.1 eV, comes from studying the shape of the energy spectrum of electrons emitted in the tritium decay, $^3\mathrm{H} \rightarrow {}^3\mathrm{He}\ e^-\nu_e$.[6] The high energy part of the energy spectrum of the electron depends on the ν_e mass. An example of the energy spectrum, called a Kurie or Fermi plot is shown in Figure 3. The Fermi plot is the decay probability, $\sqrt{N/p^2F}$, versus the electron energy, where N is the number of ^{3}H elements that decay in a given time, p is the momentum of the electron and F is a Coulomb correction factor. The Coulomb factor takes into account the energy lost (e^-) or gained (e^+) from the nuclear Coulomb field, and is important for low-energy electrons (positrons) and nuclei with large Z.[7] For $m_\nu = 0$, the energy spectrum

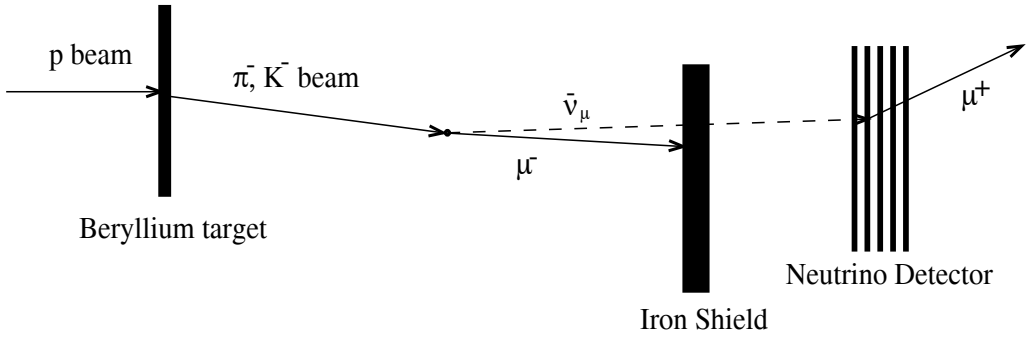

Figure 2: Schematic diagram of the muon antineutrino detection experiment performed by Lederman *et. al.* at the Brookhaven National Laboratory, where the neutrino detector is composed of spark chambers sandwiched between aluminum plates.

crosses the x-axis at $E = E_0$, where E_0 is the maximum energy available for the decay (the dashed line in Figure 3(a)). If $m_\nu > 0$, then the spectrum is modified at large electron energies so that it crosses the x-axis at $E = E_0 - m_\nu c^2$ (the solid line in Figure 3(b)). The observed shift can be used to obtain a measure of the neutrino mass. The situation is more complicated in practice with detector resolutions degrading the endpoint of the energy spectrum (see Figure 3(b)). The results of two tritium beta-decay experiments are shown in Figures 4(a) and (b). The experiment by Bergkvist gave a mass limit of 67 eV in 1972[8] while four years later Tretyakov *et. al.* lowered the limit on m_{ν_e} to 40 eV.[9] Experiments have since used new detectors and new techniques that have reduced these limits substantially to 5.1 eV.[6]

The mass of the ν_μ is measured by studying the $\pi^+ \rightarrow \mu^+\nu_\mu$ decay. The first such limit was obtained in 1956 by Barbas and collaborators at the 184-inch cyclotron at the Lawrence Berkeley Laboratory.[10] When the pion decays at rest, the mass of the muon neutrino, m_{ν_μ}, is

$$m_{\nu_\mu}^2 = m_\pi^2 + m_\mu^2 - 2m_\pi\sqrt{p_\mu^2 + m_\mu^2}, \tag{1}$$

where m_π and m_μ are the pion and muon masses, respectively, and p_μ is the momentum of the muon decay product. Experiments measure the muon momentum as it travels away from the decay point of the pion. In a recent measurement by Assamagan *et. al.*,[11] the momentum was measured in a magnetic spectrometer that contained a muon detection system composed of a silicon microstrip detector. The precision of this measurement ($p_\mu = 29.79207 \pm 0.00012$ MeV/c) and the uncertainty in the pion mass ($m_\pi = 139.56995 \pm 0.00035$ MeV) and muon mass ($m_\mu = 105.658389 \pm 0.000034$ MeV)

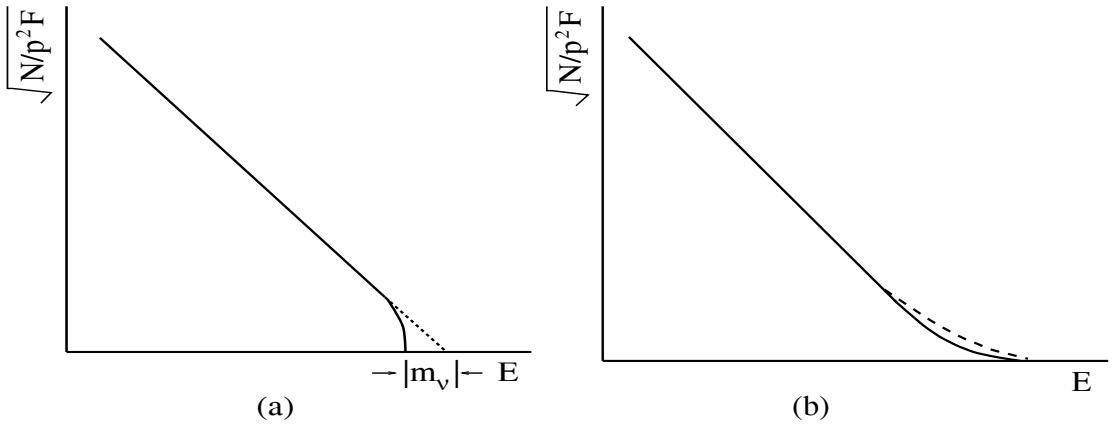

Figure 3: An example of a Kurie or Fermi plot for a detector with (a) perfect resolution, (b) finite resolution. E is the electron energy and $(N/p^2F)^{1/2}$ is the tritium decay probability, where N is the number of ^{3}H elements that decay in a given time, p is the momentum of the electron and F is the Coulomb correction factor. The solid line is the expected energy spectrum for neutrinos with $m_\nu > 0$ while the dashed line is the energy spectrum when $m_\nu = 0$.

measurements determine the best upper limit of m_{ν_μ} to be 0.16 MeV.[11] Experiments involving the $\pi^+ \rightarrow \mu^+\nu_\mu$ decay are approaching the limit set by the present experimental techniques in measuring m_π, m_μ and p_μ. New approaches that could improve the measurement of m_{ν_μ} include: studying the decay-in-flight of pions and kaons, interactions involving ν_μ, and radiative pion decay experiments.[12]

The mass of the ν_τ can be determined directly by studying the properties of tau decays, and can be inferred indirectly from the standard model or from astrophysical and cosmological models. Direct measurements of the tau neutrino mass are made by studying the properties of the decay products of the tau. The tau decay modes have the general form $\tau^- \rightarrow X^-\nu_\tau$, where due to the large mass of the tau, 1777 MeV, the X^- can be composed of lepton pairs ($e^-\nu_e$ or $\mu^-\nu_\mu$) or hadrons (pions or kaons). If the initial momentum of the tau is known and the energy and momentum of the decay products can be measured, then a limit can be placed on the mass of the tau neutrino. The best estimate of m_{ν_τ} was calculated using this method; the ALEPH collaboration studied the $\tau^- \rightarrow 3\pi^- 2\pi^+(\pi^0)\nu_\tau$ decay and measured m_{ν_τ} to be less than 24 MeV.[13] Direct measurements of m_{ν_τ} will be discussed further in Section 2 while indirect measurements of m_{ν_τ} will be discussed in Section 3.

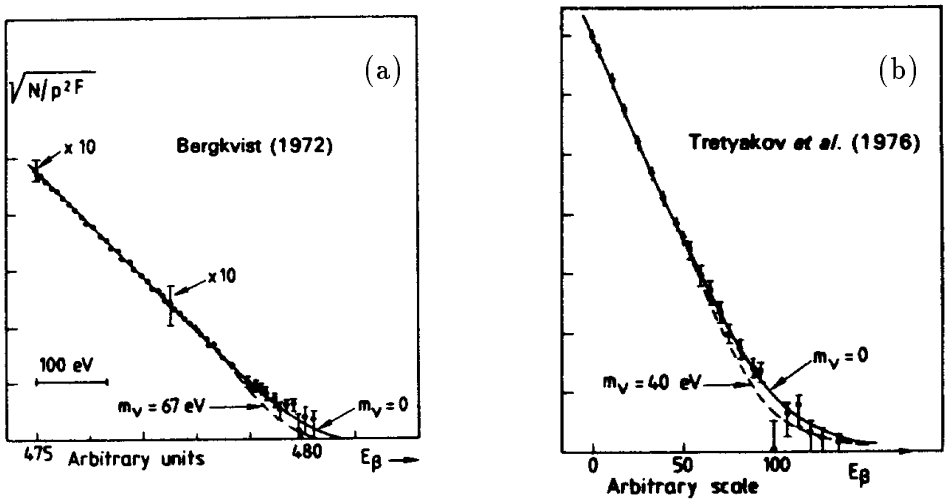

Figure 4: Kurie plots of measurements of the tritium beta-decay experiments performed by Bergkvist and Tretyakov *et. al.* [7].

1.2. The Standard Model

The Standard Model[14] is a highly successful description of the interactions of elementary particles. In this theory, matter is composed of point-like spin 1/2 fermions, which interact via the strong, weak and electromagnetic forces. These forces arise through the exchange of spin 1 particles called gauge bosons. Some properties of these gauge bosons and fermions are shown in Table 1.[6] Fermions can be categorized as either leptons or quarks based on how they interact with the three forces. Leptons consist of three charged particles: the electron (e), muon (μ) and the tau (τ); and three neutral particles: the electron neutrino (ν_e), muon neutrino (ν_μ) and the tau neutrino (ν_τ). These particles possess integer electric charge and do not interact with the strong force. There are six quarks (u,d,c,s,t and b) which have a fractional electric charge and interact via the strong force as well as the weak and electromagnetic forces. Each fermion is associated to an antiparticle with opposite electric charge and other quantum numbers. Fermions are further categorized into three families, each consisting of a lepton and quark isospin doublet. Each family consists of a pair of quarks with charges +2/3 and -1/3, a charged lepton and a neutrino. The weak force is able to couple members of each doublet to one another by charged current interactions.

Fermions (spin = 1/2)

Flavour	Mass (GeV)	Flavour	Mass (GeV)	Flavour	Mass (GeV)	Charge (Q)	Isospin T_3
$\begin{pmatrix} \nu_e \\ e \end{pmatrix}$	$< 5.1 \times 10^{-9}$ 5.1×10^{-4}	$\begin{pmatrix} \nu_\mu \\ \mu \end{pmatrix}$	$< 2.7 \times 10^{-4}$ 0.106	$\begin{pmatrix} \nu_\tau \\ \tau \end{pmatrix}$	< 0.031 1.777	0 -1	$+1/2$ $-1/2$
$\begin{pmatrix} u \\ d \end{pmatrix}$	$\sim 4 \times 10^{-3}$ $\sim 7 \times 10^{-3}$	$\begin{pmatrix} c \\ s \end{pmatrix}$	~ 1.5 ~ 0.15	$\begin{pmatrix} t \\ b \end{pmatrix}$	~ 174 ~ 4.7	$+2/3$ $-1/3$	$+1/2$ $-1/2$

Gauge Bosons (spin = 1)

Name	Charge	Mass (GeV)
photon (γ)	0	0
W^-	-1	80.22
W^+	$+1$	80.22
Z^0	0	91.19
gluon (g)	0	0

Table 1: Boson and fermion properties.

The gauge bosons mediating the strong, weak and electromagnetic forces arise due to the invariance of the Standard Model Lagrangian under a $SU(3)_c \times SU(2)_L \times U(1)_Y$ local gauge transformation. The $SU(3)_c$ group determines the couplings between strongly interacting particles by the exchange of colour carrying gauge bosons called gluons. The $SU(2)_L \times U(1)_Y$ gauge group produces the unified electroweak interaction described by Glashow, Salam and Weinberg.[15] The subscript L on $SU(2)_L$ is due to the experimental observation that the charged currents in weak interactions couple only to the left-handed chiral states of particles. The weak hypercharge Y is related to the electric field Q and the third component of the weak isospin T_3 by $Q = T_3 + Y/2$.

The masses of the gauge bosons and fermions are the result of couplings between the gauge or fermion fields and a scalar field called a Higgs field. The Higgs interaction is one way to generate particle masses in a gauge invariant, Lorentz invariant and renormalisable way. The Higgs field spontaneously breaks the local $SU(2)_L \times U(1)_Y$

gauge symmetry to produce the separate electromagnetic and weak forces. The resulting massive gauge bosons, $W^{\pm}$ and Z^0, are associated with the weak interaction, while the photon (γ), which is associated with the residual remaining unbroken $U(1)_Q$ symmetry, remains massless. The absence of right-handed neutrinos, ν_R, prevents the appearance of a Dirac mass for the neutrinos. The accidental global symmetry, $U(1)_{Y=B-L}$, corresponding to the baryon number minus the lepton number, prevents the appearance of all Majorana masses for neutrinos. Thus neutrinos are massless in the Standard Model.[16] Consequently, in order for neutrinos to have mass, extensions to the Standard Model are required.

1.3. Standard Model Extensions

Extensions to the Standard Model can involve two general types of Lorentz-invariant neutrino mass-terms: *Dirac* and *Majorana*.[14,16] Dirac neutrinos have different antiparticles, in analogy to the K^0 and $\overline{K^0}$, whereas Majorana neutrinos are identical to their antiparticles, in analogy to the π^0. Extensions to the Standard Model that allow non-zero neutrino masses add new particles: a right-handed neutrino and/or an extra boson. If the neutrinos are of the Majorana type, then they introduce a violation of lepton number (L) into the Standard Model.

The Standard Model is most often expanded to include massive neutrinos by adding a neutrino mass term to the present Standard Model Lagrangian. When both Majorana and Dirac masses are present, the massive fermions are expected to be Majorana particles. The most general neutrino mass term that includes both right and left handed neutrinos is,[6,16]

$$\frac{1}{2}(\overline{\nu}_L, \overline{\nu}_L^C) \begin{pmatrix} M_L & M_D \\ M_D & M_R \end{pmatrix} \begin{pmatrix} \nu_R^C \\ \nu_R \end{pmatrix} + \text{h.c.}, \tag{2}$$

where M_D is a Dirac neutrino mass matrix, M_L and M_R are left and right handed Majorana neutrino mass matrices, ν_R and ν_L are the right and left handed neutrino vectors, while ν_R^C and ν_L^C are the CP-conjugates of ν_L and ν_R, respectively. This expression is valid for any number of flavours and is symmetric. If as experiments show, that there are only three neutrino species,[6] then M_L, M_R and M_D are 3×3 matrices with m_L, m_R and m_D representing the individual elements of each matrix, respectively, while ν_L and ν_R are three-dimensional vectors, *i.e.* $\nu_L = (\nu_{e_L}, \nu_{\mu_L}, \nu_{\tau_L})$.

This general extension of the Standard Model has been used to develop models to predict the mass of the three neutrinos. The most popular method used to generate a neutrino mass is the so-called see-saw model. This model consists of making one particle light at the expense of making another heavy.[16,17] In order to accomplish this, the see-saw model requires that all the elements of M_L be approximately of order zero, all the elements of M_D be of the order of $m_{fermion}$, where $m_{fermion}$ is the mass of the individual leptons or quarks, while all the elements of M_R may obtain arbitrarily large values. Most see-saw models define the elements of M_R to be of order M_{GUT}, the Grand Unified Mass (GUT) scale. This is the energy value where the three running coupling constants, corresponding to the groups $SU(3)$, $SU(2)$ and $U(1)$, become equal. Current estimates of M_{GUT} give it values of order 10^{14} GeV. Harari[4] states that the elements of M_R must be much larger than the elements of M_L, *i.e.* $m_L \ll m_R$, in order to preserve the Weinberg relation, $M_W = M_Z \cos\theta_W$, where M_W and M_Z are the masses of the $W^{\pm}$ and Z^0 bosons, respectively, and θ_W is called the Weinberg angle.

Using the above assumptions for the see-saw model, the mass matrix has the form

$$\begin{pmatrix} \mathbf{0} & M_D \\ M_D & M_R \end{pmatrix}, \tag{3}$$

where M_D, M_R and $\mathbf{0}$ are 3×3 matrices. Diagonalisation of this matrix gives light-mass eigenstates with mass m_D^2/m_R and heavy-mass eigenstates with mass m_R. In the case of three generations, this would translate into three light-mass and three heavy-mass neutrinos.

In some see-saw models,[17] the neutrino mass is predicted to be proportional to the square of the mass of a fermion from the same family. For example,

$$m_{\nu_e} : m_{\nu_\mu} : m_{\nu_\tau} = m_e^2 : m_\mu^2 : m_\tau^2. \tag{4}$$

Thus according to this model the ν_e is the lightest neutrino and ν_τ is the heaviest neutrino. Substituting in the corresponding fermion masses, the light neutrinos will have a mass in the range 10^{-9} – 10^{-4} eV;[17] these values can change substantially depending on the value assigned to M_{GUT}.

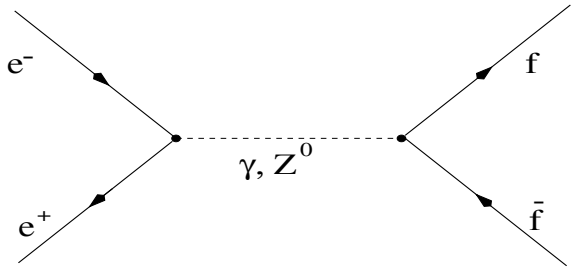

Figure 5: Feynman diagram of the $e^+e^- \rightarrow f\overline{f}$ interaction, where f is a fermion (lepton or quark).

2. Mass Limits from Tau Decays

A measurement of the mass of the tau neutrino can be made by studying the decay of the tau lepton. The first part of this section describes how taus are produced at e^+e^- colliders. In the second section, the types of detectors used to observe the decay products of the tau are reviewed. The third section will review early measurements of m_{ν_τ}. Finally, the current techniques used to estimate the tau neutrino mass are described and the limits from various collaborations are presented.

2.1. Tau Production and Decay

The tau lepton was discovered in 1975 by Perl *et. al.* from the $e^+e^- \rightarrow \tau^+\tau^-$ reaction.[18] It is the heaviest known lepton, and is sufficiently massive that it can decay to electrons, muons or hadrons. Taus are usually produced at electron-positron colliders although they can be produced at hadron machines (fixed target or colliding) where they are more difficult to identify due to the large hadronic background present in the interactions. In general, an e^+e^- collision can produce any fermion-antifermion ($f\overline{f}$) pair as long as $m_f < E_{CM}/2$, where $E_{CM} = E_{e^+} + E_{e^-}$ and f can be either a lepton or a quark. Schematically this interaction can be represented by a Feynman diagram, as shown in Figure 5.

The $e^+e^- \rightarrow \tau^+\tau^-$ cross section as a function of the centre-of-mass energy is shown in Figure 6. It can be observed that there are two energy ranges (approximately 4–12 GeV and 88–92 GeV) that would give an abundant tau sample for measurements of the properties of the τ and ν_τ. The Cornell e^+e^- storage ring (CESR) and the DESY

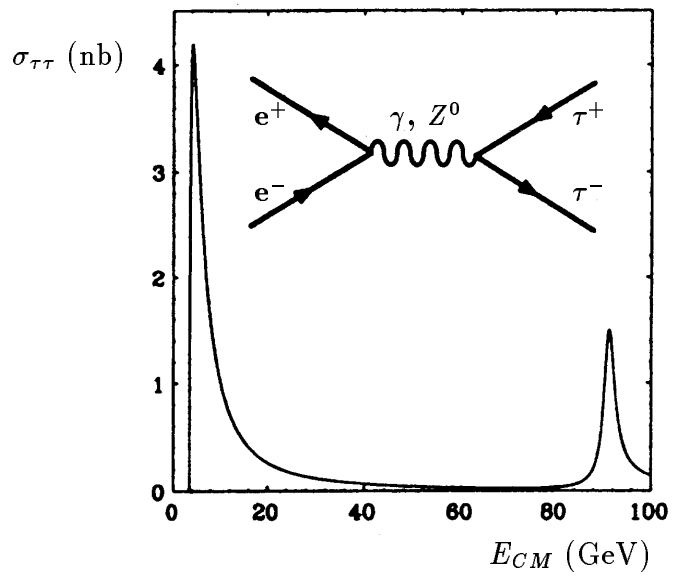

Figure 6: Total cross section for $e^+e^- \rightarrow \tau^+\tau^-$ collisions verses E_{CM}, the centre-of-mass energy, including mass and radiative corrections.[5]

e^+e^- storage ring (DORIS) produced taus at a centre-of-mass energy of $\sim$ 10.6 GeV, near the Υ(4s) resonance. Currently, the CLEO collaboration at CESR is the only experiment still taking tau data as the ARGUS collaboration at DORIS stopped collecting data in 1993. The LEP e^+e^- storage ring at CERN produced taus at or near the Z^0 mass resonance (91 MeV). The four LEP experiments, ALEPH, OPAL, DELPHI and L3, are currently analysing their data after ending tau data collection in 1995. Several other collaborations have also studied the properties of the τ and ν_τ. Table 2 gives a list of the facilities, detectors and experiments that have made measurements of the mass of the tau or tau neutrino.

Tau physics analyses require that the tau sample be as pure as possible. At the e^+e^- colliders, the $\tau^+\tau^-$ events can be easily separated from the other $f\overline{f}$ events (e^+e^-, $\mu^+\mu^-$ and $q\overline{q}$). A tau will decay into a state with either one or two neutrinos, *i.e.* $\tau^- \rightarrow X^-(\overline{\nu}_x)\nu_\tau$, where X^- is defined to be either an e^-, μ^- or $(Nh)^-$ with $N \geq 1$ and where h represents a π or K. These neutrinos are not observed in the detector and therefore generate missing energy from the event. Thus the $e^+e^- \rightarrow e^+e^-$ background, for example, can be eliminated by removing events where the full centre-of-mass energy is observed in the detector.

Laboratory	Accelerator	Experiment	E_{CM} (GeV)	$\sigma_{\tau^+\tau^-}$ (nb)	Luminosity (pb^{-1})	$N_{\tau^+\tau^-}$
CERN	LEP	OPAL[19] ALEPH[20] DELPHI[21] L3[22]	91	1.18	140	165,000
SLAC	PEP	HRS[23]	29	0.1	300	30,000
DESY	DORIS	ARGUS[24]	10	0.95	341	325,000
Cornell	CESR	CLEO[25]	10	0.92	1920	1,770,000
Beijing	BEPC	BES[26]	4	threshold	5	25,000
SLAC	SPEAR	MARK II[27]	4	2.8	21	58,600
SLAC	SPEAR	DELCO[28]	4	2.8	0.2	594

Table 2: Experiments that have made measurements of the mass of the tau or tau neutrino. Note that the MARK II and DELCO experiments also collected data using the PEP accelerator using $E_{CM} = 29$ GeV.

The $e^+e^- \rightarrow \mu^+\mu^-$ background can be eliminated by observing the presence of two high-momentum, back-to-back, charged particles that deposit very little energy in the detector. The other large background are $e^+e^- \rightarrow q\overline{q}$ events, where the quarks hadronize. The hadron multiplicity increases with energy, thus the LEP experiments at $E_{CM} = 91$ GeV can reduce the hadronic background by requiring a very limited number of charged particles (usually 6) in the final state. At ARGUS and CLEO, where the centre-of-mass energy is 10 GeV, the hadron multiplicity is low enough that the *one-prong* tag technique is needed.[24,25] This technique requires that one of the fermions in an $e^+e^- \rightarrow f\overline{f}$ reaction be identified as a tau decay to a state with only one charged track. This reduces the efficiency for finding taus, but the large data samples at ARGUS and CLEO allow them to retain a substantial tau data set.

The large mass of the tau lepton allows it to decay into several different particles, *i.e.* electrons, muons and hadrons. The various tau decays are divided into several different categories depending on the number of charged particles in the final state. For example, if there is only one charged particle in the final state then that decay is defined as a one-prong decay, similarly three charged tracks is a three-prong decay, etc. Table 3 lists these branching ratios for the one to seven prong tau decays, the various branching ratio measurements are a world average as computed by the Particle Data Group.[6]

Tau Decay	Branching Ratio
1-prong	
$\tau^- \to e^- \bar{\nu}_e \nu_\tau$	$17.88 \pm 0.18\%$
$\tau^- \to \mu^- \bar{\nu}_\mu \nu_\tau$	$17.46 \pm 0.25\%$
$\tau^- \to h^- \geq 0\pi^0 \nu_\tau$	$48.9 \pm 0.6\%$
3-prong	
$\tau^- \to 2h^- h^+ \nu_\tau$	$8.39 \pm 0.31\%$
$\tau^- \to 2h^- h^+ \geq 0\pi^0 \nu_\tau$	$5.53 \pm 0.30\%$
5-prong	
$\tau^- \to 3h^- 2h^+ \nu_\tau$	$(7.1 \pm 0.9) \times 10^{-4}$ %
$\tau^- \to 3h^- 2h^+ \geq 0\pi^0 \nu_\tau$	$(3.2 \pm 0.8) \times 10^{-4}$ %
7-prong	
$\tau^- \to 4h^- 3h^+ \geq 0\pi^0 \nu_\tau$	$\leq 1.9 \times 10^{-4}$ % (90% C.L.)

Table 3: The world average tau lepton branching ratios as calculated by the Particle Data Group.[6] Note that *prong* labels the number of charged particles from the tau decay and that h^- represents either π^- or K^-.

2.2. Detectors

The particle detectors used to observe tau decay properties have a similar general design. The detectors have a central tracking chamber, which can be composed of a silicon microvertex detector, a drift chamber and/or a time projection chamber. The tracking chamber is immersed in a magnetic field created by a solenoid so that a measure of the resulting curvature of a particle trajectory gives a measure of the particle's momentum. The tracking chamber can also measure the energy loss of a particle as it passes through the detector. Outside of the central tracking chamber are the electromagnetic and hadronic calorimeters. The electromagnetic calorimeter is used to contain and measure the energy of electrons, positrons and photons, whereas the hadron calorimeter contains and measures the energy of the hadrons. Finally, muon chambers are placed around the outside of the detectors to observe any charged particles, particularly muons, that can pass through the detector without being stopped. The remainder of this section will focus on the ALEPH detector that, so far, has achieved the best limit on the mass of the tau neutrino.

The ALEPH detector (see Figure 7) is one of four at the e^+e^- collider ring known as LEP. A complete description of the ALEPH detector is described in the literature.[29]

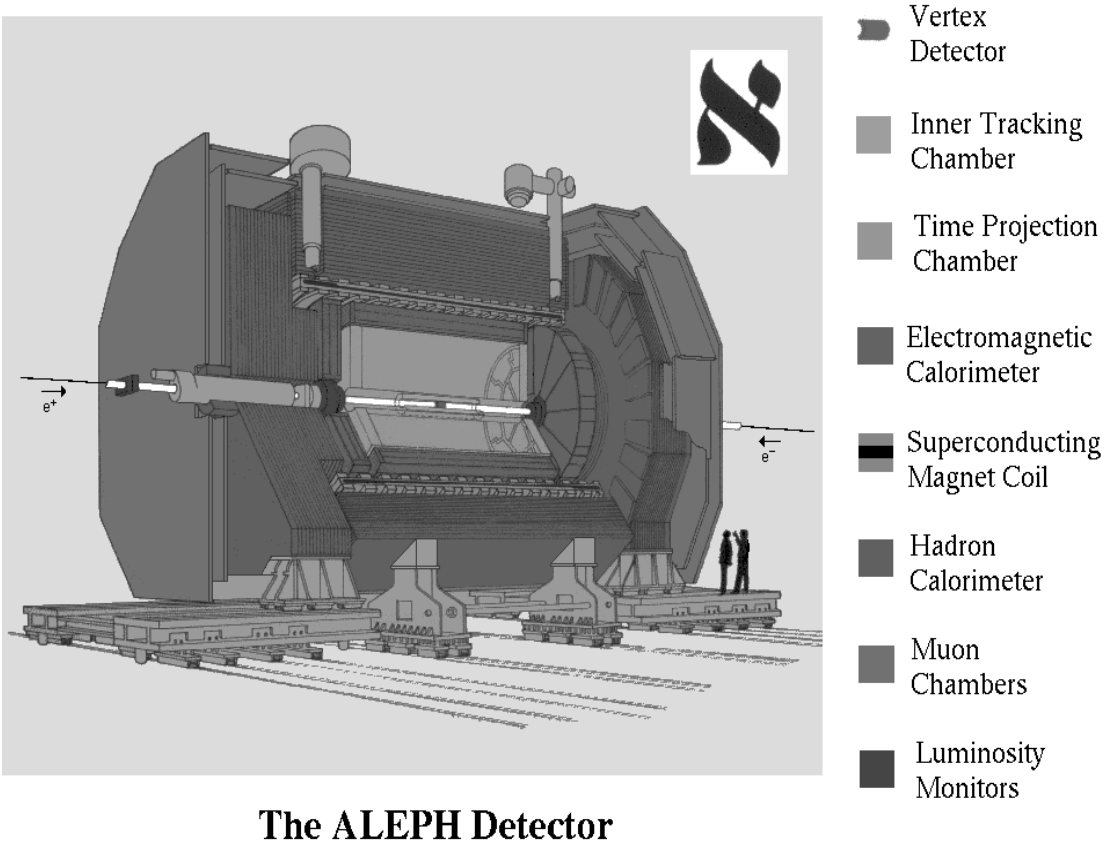

Figure 7: The ALEPH detector.[29]

The ALEPH detector measures charged particle trajectories in an axial magnetic field of 1.5 T using a silicon vertex detector with two-dimensional readout, a drift chamber and a time projection chamber (TPC). The transverse momentum resolution for high momentum particles is $\delta p_T/p_T = 6 \times 10^{-4} p_T$ GeV. The mass resolution for a multibody decay, like $D^0 \rightarrow K^-\pi^-\pi^+\pi^+$, is typically 10 MeV. Surrounding the tracking detectors are the electromagnetic calorimeter, the superconducting solenoid, the hadron calorimeter and the muon chambers. The electromagnetic calorimeter (ECAL) is made out of lead-wire chambers with a cathode-pad read-out arranged in $0.9^\circ \times 0.9^\circ$ projective towers divided in three longitudinal segments. The ECAL has an energy resolution of $\sigma_E/E = 0.18\sqrt{E(\mathrm{GeV})} + 0.009$. The hadron calorimeter is composed of 1.2 m of iron, interleaved with 23 layers of streamer tubes, while the muon chambers consists of two double layers of streamer tubes. Charged particle (*eg.* electrons, muons or hadrons) identification is performed with a maximum likelihood method using the combined information from all subdetectors.[30]

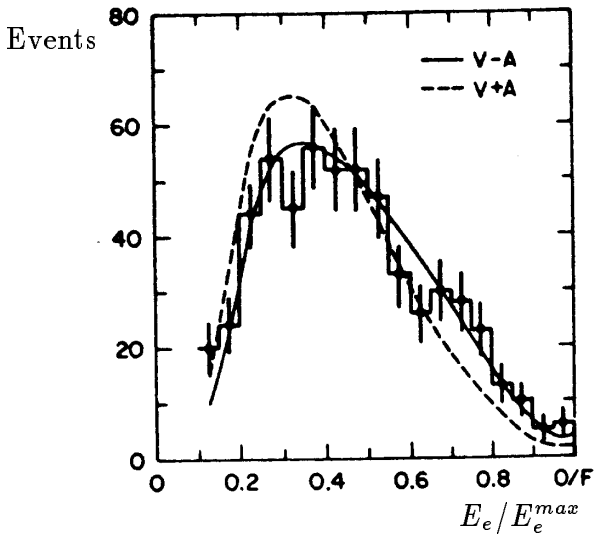

Figure 8: The DELCO momentum spectra for the $\tau^- \rightarrow e^-\bar{\nu}_e\nu_\tau$ decay,[28] where E_e is the electron energy and E_e^{max} is the maximum available energy for the electron. The solid and dashed lines are, respectively, $V - A$ and $V + A$ fits to the data when m_{ν_τ} has zero mass.

2.3. Early Measurements

The first measurement of the mass of the tau neutrino was made by the DELCO collaboration which measured the electron energy spectrum from $\tau^- \rightarrow e^-\bar{\nu}_e\nu_\tau$ decays (see Figure 8). They fit the spectrum with theoretical predictions assuming different values of m_{ν_τ} and observed that m_{ν_τ} had to be less than 250 MeV.[28] This technique is limited by the size of the tau sample and energy resolution of the detector. A recent study by Gomez-Cadenas and Gonzalez-Garcia proposed that m_{ν_τ} could be measured at a high luminosity tau factory using a high resolution detector; but even then, the tau neutrino mass bound could only be reduced to between 20 and 40 MeV.[31] Consequently, studies to improve the limit on the tau neutrino mass concentrated on the tau hadronic decay modes.

2.4. Current Measurement Techniques

Several experiments have measured the tau neutrino mass from tau hadronic decays. These decay modes can have several particles in the final state, *i.e.* $\tau^- \rightarrow X^-\nu_\tau$, where $X^- \equiv (Nh)^-$, $N \geq 1$ and h is either a π or K. Consequently, tau hadronic decays with high multiplicities are expected to have some events that will be close to the kinematically allowed end-point of the hadronic energy spectrum, in other words, a very low energy neutrino. A fit to a theoretical spectrum via the maximum likelihood technique can be used to set a limit on m_{ν_τ}. Although this method makes use of the entire spectrum, its sensitivity comes from the events with m_X and E_X closest to the end-point. Thus a single observed event may be sufficient to constrain the neutrino mass. These measurements are limited by the experimental resolution of the mass and energy of the tau and its decays products, hence it is critically important to suppress backgrounds, since the mass of the background events can appear to be very close to or even above m_τ.

The details of two methods used to set a limit on m_{ν_τ} from tau decays will be discussed below. A summary of the published limits on the tau neutrino mass from tau decays is shown in Figure 9. As can be observed, the limit has been reduced over the last fifteen years as new techniques and different tau decays have been studied.

2.4.1. One-dimensional Method

The one-dimensional method determines m_{ν_τ} from the spectrum of the invariant mass of the tau decay products m_X. This measurement is most sensitive to events with $m_X \sim m_\tau$, since this is where the spectrum varies most dramatically as a function of m_{ν_τ}. Most of the collaborations have used the one-dimensional method to calculate a limit on m_{ν_τ}, the exceptions include OPAL,[19,32] which use a two-dimensional method, and ALEPH,[20] which use the combination of the one and two-dimensional methods. The remainder of this section will focus on the best one-dimensional measurement which was made by the ARGUS collaboration.

The ARGUS collaboration use the $\tau^- \rightarrow 3\pi^-2\pi^+\nu_\tau$ decay to estimate a limit on m_{ν_τ}.[24] The limit is based on an initial data sample of 325,000 tau-pairs collected at a centre-of-mass energy of $\sim$10 GeV. The data sample is selected using the *one-prong* method, as described in Section 2.1. A second selection to identify the $\tau^- \rightarrow 3\pi^-2\pi^+\nu_\tau$

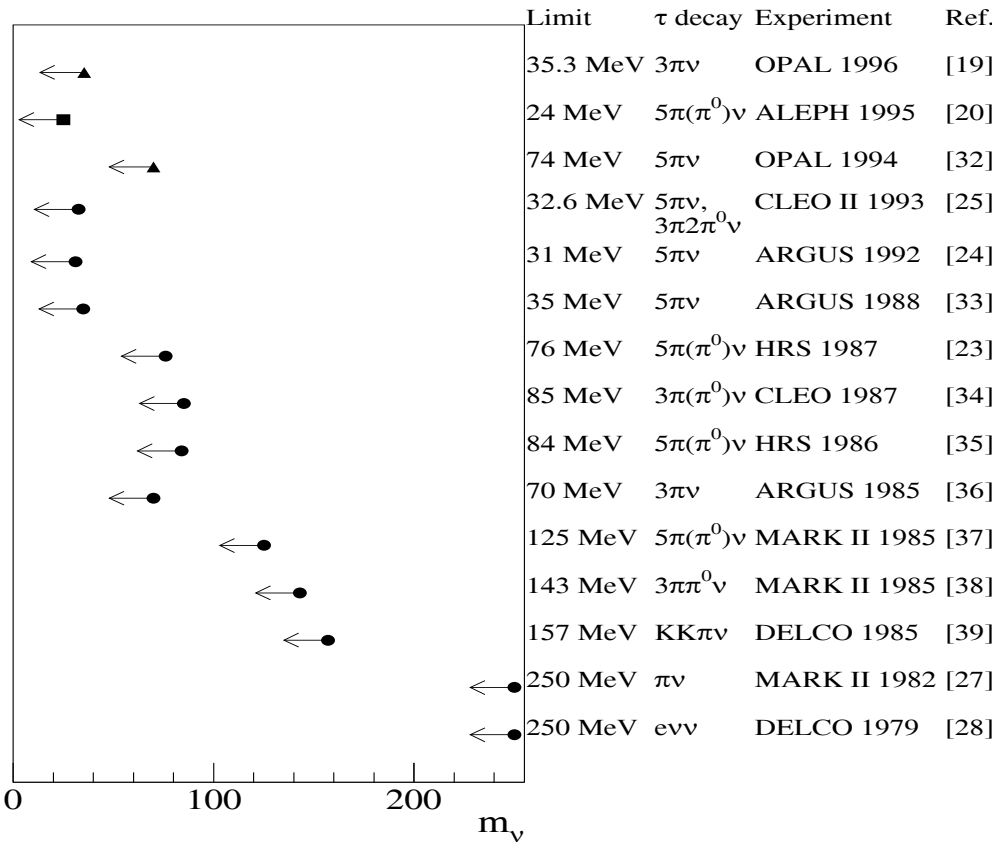

Figure 9: Summary of published tau neutrino mass limits from various tau decays. The MARK II and DELCO quote limits at the 90% confidence level while the other experiments quote limits at the 95% confidence level. The OPAL measurements use the two-dimensional method, ALEPH uses a combination of the one and two-dimensional methods and the remainder of the measurements use the one-dimensional method.

decays was performed giving 20 events. The background of the data sample was estimated to be less than one event.[24]

The tau neutrino mass limit is determined by a maximum likelihood function which consists of the expected mass distribution of the five-pion invariant mass distribution convoluted with the detector and mass resolutions, and the acceptance functions. Note that the integral only includes neutrino masses that are positive. The mass resolution and acceptance functions are determined by simulated event samples. The mass resolution of the decay products in the $\tau^- \to 3\pi^- 2\pi^+ \nu_\tau$ decay is typically 20 MeV. The distribution obtained by ARGUS is shown in Figure 10,[24] where the solid

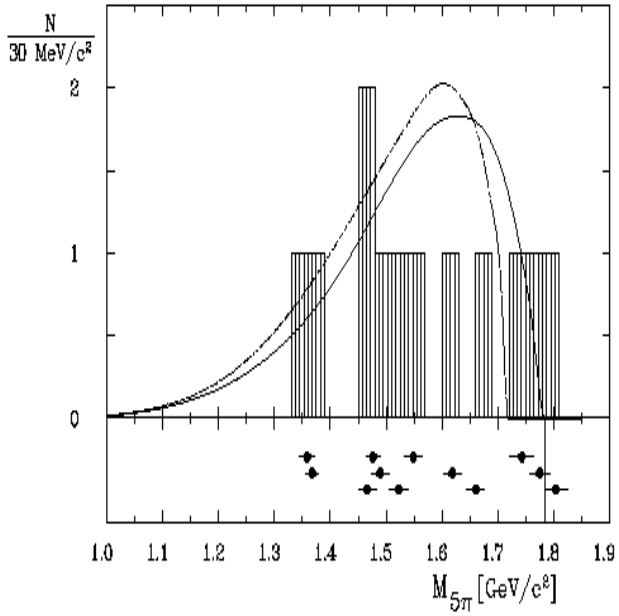

Figure 10: A histogram of the invariant masses $m_{5\pi}$ (equivalently, m_X) measured in the $\tau^- \to 3\pi^- 2\pi^+ \nu_\tau$ decay by the ARGUS collaboration.[24] The solid curve is the expected distribution for m_X at $m_{\nu_\tau} = 0$. The dashed curve is the expected distribution for m_X at $m_{\nu_\tau} = 70$ MeV. The mass and the error on the mass for every event are shown below the histogram. The tau mass is indicated by the solid line.

curve is the expected distribution for m_X at $m_{\nu_\tau} = 0$, the dashed curve is the expected distribution for m_X at $m_{\nu_\tau} = 70$ MeV, and underneath, the distribution the mass and the error on the mass for each event are shown with the tau mass indicated by the solid line.

The likelihood is calculated event by event as a function of m_{ν_τ}, and the final likelihood is a product of these individual event likelihoods. The result is corrected for systematic errors present in the event sample, including the uncertainty in the tau mass, underestimation of the mass resolution, uncertainty in the momentum due to other decays and uncertainty in the theoretical decay model. The final result from ARGUS using the one-dimensional method for the $\tau^- \to 3\pi^- 2\pi^+ \nu_\tau$ decay gave $m_{\nu_\tau} <$ 31 MeV[24] (see Figure 9).

2.4.2. Two-dimensional Method

The two-dimensional mass method can achieve a better discrimination between the different m_{ν_τ} hypotheses by exploiting both the distribution of the invariant mass, m_X, and energy, E_X, of the tau decay. In the centre-of-mass frame of the tau, the energy and momentum of the decay products (X^-) can be written as

$$\begin{aligned} E'_X &= \frac{m_\tau^2 + m_X^2 - m_{\nu_\tau}^2}{2m_\tau} \\ |\vec{p}|' &= \frac{\sqrt{(m_\tau^2 - (m_X + m_{\nu_\tau})^2)(m_\tau^2 - (m_X - m_{\nu_\tau})^2)}}{2m_\tau}. \end{aligned} \quad (5)$$

Since the tau is not at rest, a Lorentz transformation from the tau rest frame into the laboratory frame must be performed to obtain the energy in the laboratory frame,

$$\begin{aligned} E_X &= \gamma E'_X + \gamma\beta|\vec{p}|'\cos\theta' \\ &= \gamma\frac{m_\tau^2 + m_X^2 - m_{\nu_\tau}^2}{2m_\tau} + \gamma\beta\frac{\sqrt{(m_\tau^2 - (m_X + m_{\nu_\tau})^2)(m_\tau^2 - (m_X - m_{\nu_\tau})^2)}}{2m_\tau}\cos\theta' \end{aligned} \quad (6)$$

where $\gamma = \frac{E_{beam}}{m_\tau}$, $\beta = \sqrt{1 - \frac{1}{\gamma^2}}$ and $\cos\theta'$ is the angle between the tau and X directions in the laboratory system. This distribution now combines the mass and energy inequalities and thus forms the basis for the two-dimensional method used to measure the tau neutrino mass.

A plot of the distribution of E_X versus m_X is shown in Figure 11 for a tau with $E_\tau = 45$ GeV. The curves in the plot, obtained from equation (6), enclose the kinematically allowed or accessible region for any particular tau decay. Each curve represents a given neutrino mass, as labeled just inside the respective curve. The extent of the accessible region decreases with increasing neutrino mass. Using the highest multiplicity (3π or 5π) events increases the population in the high mass region of the plot where the variation with m_{ν_τ} is maximal.

The first collaboration to utilize the two-dimensional technique was the OPAL collaboration[32] using $\tau^- \to 3\pi^- 2\pi^+ \nu_\tau$ decays. In 1995 OPAL[19] made a new measurement of m_{ν_τ} using $\tau^- \to 2\pi^-\pi^+\nu_\tau$ decays. In the same year, the ALEPH[20] collaboration achieved the best m_{ν_τ} limit by studying $\tau^- \to 3\pi^- 2\pi^+(\pi^0)\nu_\tau$ decays (see Figure 9). The remainder of this section will focus on the measurement by ALEPH.

The ALEPH analysis was based on a data sample of 65 pb^{-1} collected from 1991-1993. A total of 76,000 tau-pair events were selected using the standard ALEPH

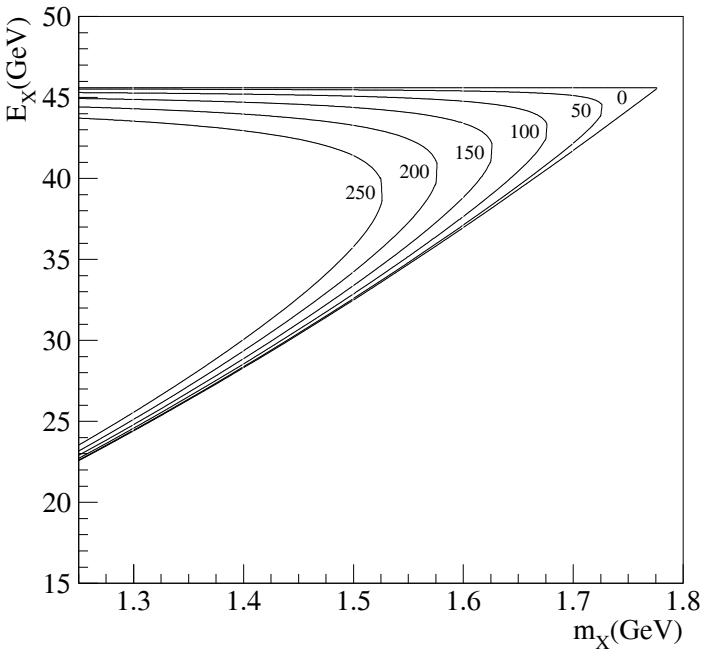

Figure 11: Distribution of the hadronic energy versus the invariant mass of the tau decay products for a tau with $E_\tau = 45$ GeV. The curves enclose the kinematically allowed region for a tau decay to occur. Each curve is plotted for a specific neutrino mass in units of MeV, as labeled just inside the respective curve.

selection procedures.[40] The efficiency within the geometrical acceptance of the detector was 93.2%. A further selection identified 23 events as $3\pi^-2\pi^+$ and 2 events as $3\pi^-2\pi^+\pi^0$ candidates. All observed events were in the 5–1 topology, where five pions were contained within one-half of the detector while a single charged particle was contained in the other half. The background contained within the 5–1 topology sample was negligible.

The ALEPH method to determine the tau neutrino mass uses an analytical maximum likelihood function that gives the probability density of obtaining the observed distribution in the plane $(x = \frac{m_{had}}{m_\tau}, y = \frac{E_{had}}{E_{beam}})$, where m_{had} is the total pion mass, m_τ is the mass of the tau, E_{had} is the energy of the pions and E_{beam} is the beam energy. Note that m_{had} and E_{had} are equivalent to m_X and E_X, respectively. The distribution of E_{had}/E_{beam} versus m_{had} is plotted in Figure 12. The kinematically allowed regions for two different neutrino masses (0 and 31 MeV) are plotted.

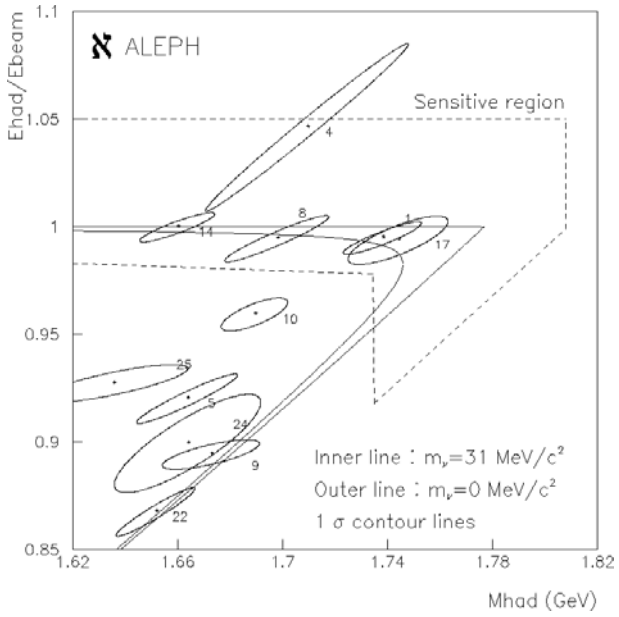

Figure 12: Distribution of E_{had}/E_{beam} versus the hadronic invariant mass of data events from ALEPH[20] in the range $m_{had} > 1.62$ GeV and $E_{had}/E_{beam} > 0.85$. The kinematically allowed regions for $m_{\nu_\tau} = 0$ MeV and 31 MeV are plotted and the sensitive region as defined in the text is drawn (dashed line).

The effects of background on the determination of the limit on m_{ν_τ} depend strongly on the position in the E_{had} *vs* m_{had} plane of the background events and on the accuracy with which that position is determined. This is a consequence of the fact that the sensitivity to m_{ν_τ} varies considerably across the plane, increasing near the border of the allowed region. The most sensitive region of the plane is shown in Figure 12 enclosed by the dashed lines. In the ALEPH analysis, the background is considered to be negligible either if it introduces a bias towards higher neutrino masses, or if it contributes less than 1% to the total number of events entering the sensitive region of the plane.

In order to get an estimation of the neutrino mass, a probability density function is constructed for any given event i,

$$P_i(m_{\nu_\tau}) = \frac{1}{N(m_{\nu_\tau})} \int_{x_0}^{x_1(m_{\nu_\tau})} dx \int_{m_\tau}^{E_{beam}} dE_\tau \mathcal{G}(\mathcal{E}_\tau) \int_{\dagger\prime(\mathcal{E}_\tau, \Updownarrow_{\nu_\tau})}^{\dagger\infty(\mathcal{E}_\tau, \Updownarrow_{\nu_\tau})} \lceil\dagger \mathcal{R}(\S - \S\rangle, \dagger - \dagger\rangle) \epsilon(\S, \dagger) \frac{-^{\in}(\S, \dagger, \Updownarrow^{\in}_{\nu_\tau})}{\lceil\S \lceil\dagger}, \tag{7}$$

where

- $\frac{\Gamma^2(x,y,m^2_{\nu_\tau})}{dxdy}$ is the theoretical distribution of the given decay mode;

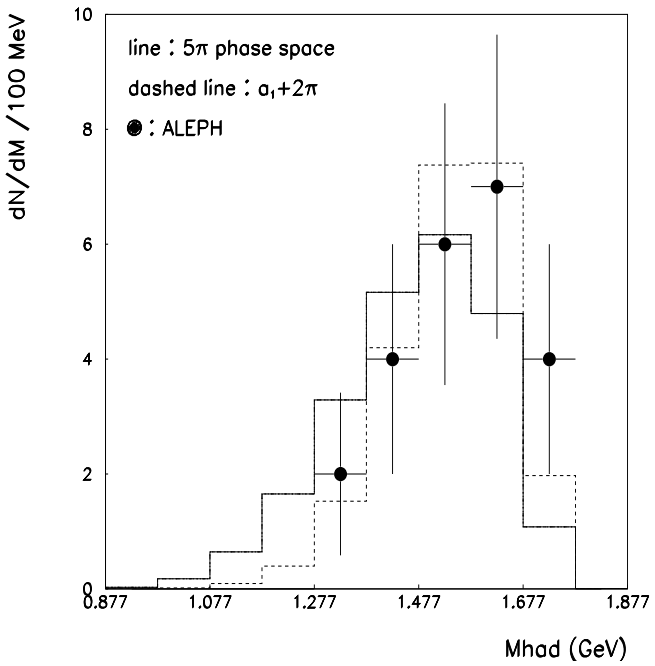

Figure 13: Invariant mass distribution of 5π data events compared with two assumptions on resonance production.

- $\epsilon(x, y)$ is the selection efficiency;
- $\mathcal{R}(\S - \S_\rangle, \dagger - \dagger_\rangle)$ is the normalized resolution function, namely a multivariate gaussian with an additional constant tail taking into account pattern recognition ambiguities in track reconstruction;
- $\mathcal{G}(\mathcal{E}_\tau)$ is the initial state radiation function;
- $\mathcal{N}(\Updownarrow_{\nu_\tau})$ is the normalization factor;
- $(y_0, y_1) = \left(\frac{E^*(1-\beta\sqrt{1-(m_{had}/E^*)^2})}{m_\tau}, \frac{E^*(1+\beta\sqrt{1-(m_{had}/E^*)^2})}{m_\tau} \right)$, where E^* is the hadronic energy in the tau rest frame and β is the tau velocity; and
- $(x_0, x_1) = \left(\frac{\sum_{i=1}^{5(6)} m_\pi}{m_\tau}, \frac{m_\tau - m_{\nu_\tau}}{m_\tau} \right)$, where m_π, m_τ and m_{ν_τ} are the masses of the pions, tau and tau neutrino, respectively.

The theoretical distribution for the $\tau^- \to 3\pi^- 2\pi^+(\pi^0)\nu_\tau$ decay, $\frac{\Gamma^2(x,y,m^2_{\nu_\tau})}{dxdy}$, is only defined in the allowed region (see Figure 12). Consequently any event falling outside the allowed region contributes to the likelihood only to extent permitted by the resolution or radiation functions. The resolution functions are determined by simulated event samples with checks performed on the data to ensure that the simulated event sample models the

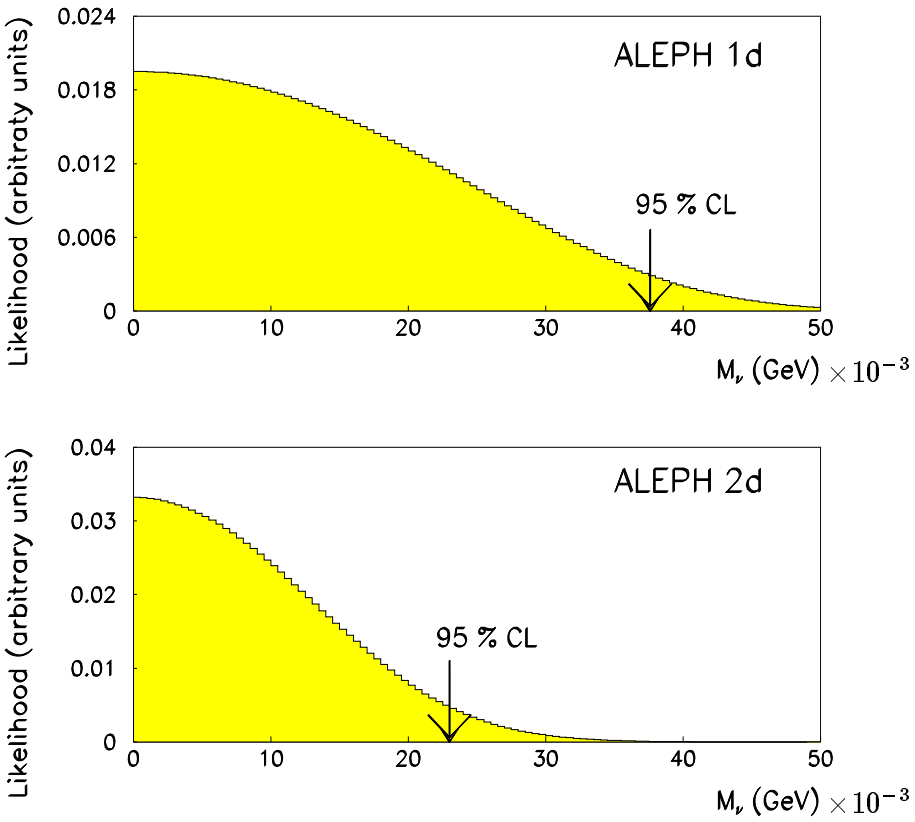

Figure 14: Total likelihood versus tau neutrino mass for the one dimensional (top) and two dimensional (bottom) fit.

data correctly. The typical mass and energy resolution for the 5π events is 15 MeV and 350 MeV while for the $5\pi\pi^0$ events is 35 MeV and 800 MeV, respectively. The mass distribution obtained by ALEPH for the 5π data is shown in Figure 13, where the points are the data and the solid and dashed lines represent two assumptions of resonance production modes.

The likelihood is calculated event by event as a function of m_{ν_τ}, and the final likelihood is a product of these individual event likelihoods. The dependence of the likelihood on the neutrino mass is shown in Figure 14 for both the one and two dimensional fits. Both fits show that the mass of the tau neutrino is compatible with zero. The m_{ν_τ} limit from the one dimensional fit gives a 95% confidence limit of 37.5 MeV and the two dimensional fit gives a limit of 23.0 MeV. Several systematic effects were then considered on each of the probability density function variables, where the total systematic error was dominated by the knowledge of the resolution functions. Therefore including the systematic errors the ALEPH m_{ν_τ} limits

are: $m_{\nu_\tau} < 40.6$ MeV at the 95% confidence level for the one-dimensional fit and $m_{\nu_\tau} < 23.8$ MeV at the 95% confidence level for the two-dimensional fit. Thus the overall upper limit from this method gives a m_{ν_τ} limit of 24 MeV at the 95% confidence level.[20]

3. Model Dependent Mass Limits

The mass of the tau neutrino can be calculated by comparing experimental measurements with theoretical expectations. The first part of this section describes how the branching ratio of the $\tau^- \to e^- \bar{\nu_e} \nu_\tau$ decay mode can be used to set a limit on m_{ν_τ}. The second part of this section describes how the supernova explosion, SN1987A, can be used to measure m_{ν_τ}. Finally, the third part of this section describes how elements of the standard model of cosmology, the energy density of the universe and nucleosynthesis, give a measure of m_{ν_τ}.

3.1. $\tau^- \to e^- \bar{\nu_e} \nu_\tau$ decays

Limits on the mass of the tau neutrino can be determined by comparing the $\tau^- \to e^- \bar{\nu_e} \nu_\tau$ decay width with the standard model prediction.[49] The width for the $\tau^- \to e^- \bar{\nu_e} \nu_\tau$ decay is well understood. The masses of the electron (0.511 MeV) and electron neutrino (≤ 5.1 eV) are small and have little influence on the decay width. Normally the mass of the tau neutrino is assumed to be zero, however, if it is not zero then the width can be written as[41,42]

$$\Gamma^{m_{\nu_\tau} \neq 0}_{\tau^- \to e^- \bar{\nu}_e \nu_\tau} = \Gamma^{m_{\nu_\tau}=0}_{\tau^- \to e^- \bar{\nu}_e \nu_\tau} f\left(\frac{m^2_{\nu_\tau}}{m^2_\tau}\right), \tag{8}$$

where

$$f(x) = 1 - 8x + 8x^3 - x^4 - 12x^2 \ln x, \tag{9}$$

$$\Gamma^{m_{\nu_\tau}=0}_{\tau^- \to e^- \bar{\nu}_e \nu_\tau} = \frac{g^4}{(8m^2_W)^2} \frac{m^5_\tau}{96\pi^3} C, \tag{10}$$

g is the charged coupling constant (assuming lepton universality), m_W and m_τ are the masses of the W and τ respectively and C represents small higher-order corrections.

The width for the $\mu^- \to e^- \bar{\nu_e} \nu_\mu$ decay has a form similar to that of the $\tau^- \to e^- \bar{\nu_e} \nu_\tau$ width. Dividing the $\tau^- \to e^- \bar{\nu_e} \nu_\tau$ width (for $m_{\nu_\tau} \neq 0$) by the $\mu^- \to e^- \bar{\nu_e} \nu_\mu$ width, it is found that

$$\frac{\Gamma(\tau^- \to e^- \bar{\nu_e} \nu_\tau)}{\Gamma(\mu^- \to e^- \bar{\nu_e} \nu_\mu)} = 1.00039 \left(\frac{m_\tau}{m_\mu}\right)^5 f\left(\frac{m^2_{\nu_\tau}}{m^2_\tau}\right) \tag{11}$$

where it is assumed that the ν_μ and ν_e are massless. Equation (11) can now be rewritten in terms of the electronic branching ratios of the tau and muon and their lifetimes, T_τ and T_μ respectively, to obtain

$$B_e \equiv B(\tau^- \to e^- \bar{\nu}_e \nu_\tau) = 1.00039 \left(\frac{m_\tau}{m_\mu}\right)^5 \frac{T_\tau}{T_\mu} f\left(\frac{m_{\nu_\tau}^2}{m_\tau^2}\right) \tag{12}$$

where $\Gamma(\tau^- \to e^- \bar{\nu}_e \nu_\tau) = B(\tau^- \to e^- \bar{\nu}_e \nu_\tau)/T_\tau$ and $\Gamma(\mu^- \to e^- \bar{\nu}_e \nu_\mu) = B(\mu^- \to e^- \bar{\nu}_e \nu_\mu)/T_\mu$. The branching ratio, lifetime and mass of the muon are well measured and are taken from the 1994 Particle Data Group Summary.[6] The tau mass of $1776.96^{+0.18+0.25}_{-0.21-0.17}$ MeV is the most recent measurement made by the BES collaboration.[26]

The average $\tau^- \to e^- \bar{\nu}_e \nu_\tau$ branching ratio of $(17.80 \pm 0.08)\%$ is calculated as a weighted average of measurements taken after 1990. Those taken prior to 1990 are less precise and have little influence on the final value. Most of the branching ratios are summarized in the Particle Data Group Summary,[6] however, three recent measurements by OPAL,[43] ALEPH[44] and DELPHI[45] are also included. The average tau lifetime of 291.0 ± 1.4 fs is calculated as a weighted averaged of measurements by the four LEP experiments,[46] CLEO[47] and SLD.[48]

In Fig. 15 the tau lifetime, the $\tau^- \to e^- \bar{\nu}_e \nu_\tau$ branching ratio and tau mass are plotted against one another. The data are best described by equation (12) when m_{ν_τ} is 25 MeV. The lines drawn in the figure represent the theoretical predictions based on equation (12) for various m_{ν_τ}. To estimate a limit on m_{ν_τ}, it was assumed that the errors on m_τ, T_τ and B_e can be modeled by independent gaussian distributions. The total probability is the product of the three gaussian distributions. Integrating over the allowed region $m_{\nu_\tau} < 71$ MeV at the 95% confidence level is achieved.[49]

3.2. Supernova explosion SN1987A

A limit on the mass of each neutrino species can be calculated from the observed difference in the arrival times of the first and last neutrino to arrive here on earth from a supernova explosion. The process of creating a supernova explosion begins with the gravitational collapse of a large star. Towards the end of a star's nuclear burning stage, it has an interior temperature of $\sim 10^9$ K with a central core mass of about 1.5 solar masses, composed mainly of iron. The atoms are fully ionized and the electrons form a degenerate gas which provides the pressure that balances gravitational attraction. Protons contained in the iron core can capture some of the electrons, leaving behind neutrons and neutrinos ($pe^- \to n\nu_e$). The core then collapses when the mass can no longer be supported by the reduced number of electrons. At some point the compression ceases and the core bounces

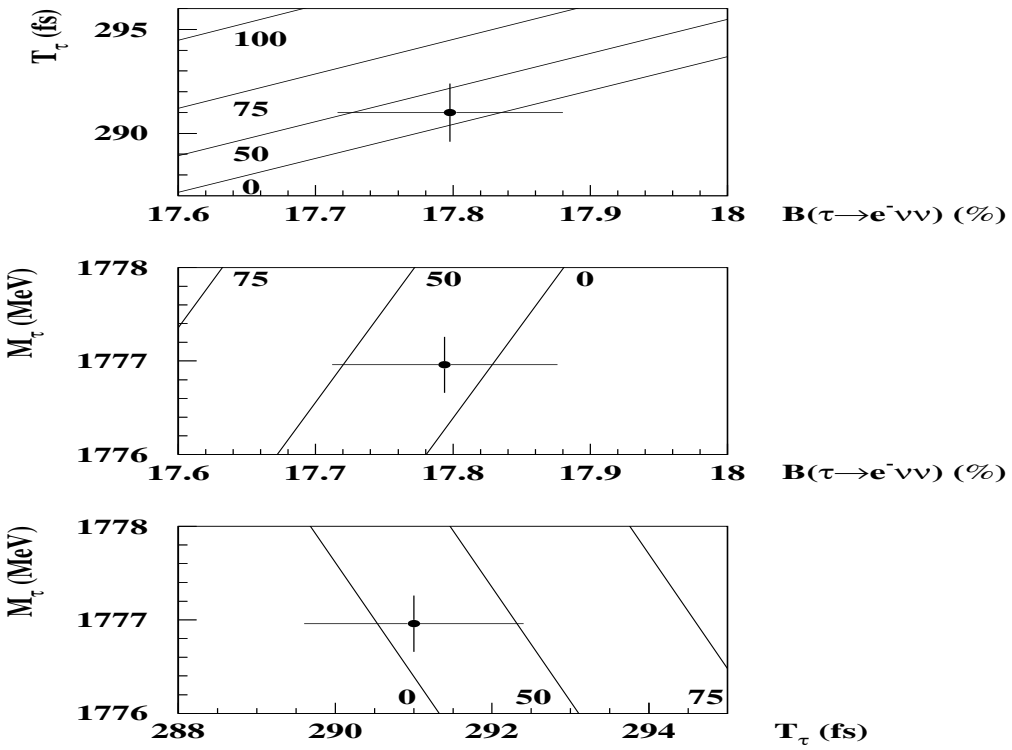

Figure 15: The tau lifetime, mass and $\tau^- \to e^- \bar{\nu}_e \nu_\tau$ branching ratio plotted against one another. The lines are the standard model prediction as described in the text where the label indicates the mass of the tau neutrino.

back resulting in outward pressure waves that collect to form a shock wave. This shock wave disrupts the star's surrounding mantle and an explosion follows, resulting in a type II supernova, if the initial mass of the star is greater than approximately 8 solar masses. The enormous store of energy in the core is released in approximately 10 seconds, in the form of neutrinos; leaving behind a neutron star.

All three types of neutrinos are produced in the explosion. Electron neutrinos are created via the electron capture reactions leading to the collapse while all three neutrino species are created from electron-positron annihilations occurring after the collapse. The electrons and positrons needed for these reactions arise from photon pair production, where the photons are created through bremsstrahlung. The initial part of the burst, of a few milliseconds duration, is expected to release mostly electron neutrinos from the electron

capture processes leading to the collapse, while the latter part of the burst contains a mixture of all three neutrino species. All the neutrinos will be emitted from the supernova explosion within a few seconds. If the neutrinos have mass, they will travel at relativistic speeds ($\beta_\nu = \sqrt{1-(m_\nu/E_\nu)^2}$) and arrive on earth at a time $T = d/\beta_\nu c$, where d is the distance between the supernova and earth. The time of the arrival between the first neutrino and the last can be used to determine a limit on the neutrino mass, such that[17]

$$\Delta t = 0.026\,\frac{d \times m}{E^2}, \tag{13}$$

where time Δt is in seconds, the mass m in eV, the energy E in units of 10 MeV and the distance d in units of 50 kpc $= 1.54 \times 10^{21}$ m.

On February 23, 1987, SN1987A, a type II supernova, was discovered at an estimated distance of 50 kpc. A neutrino burst was observed by two large water Cerenkov detectors at the Kamiokande and IMB experiments. The signal detected by the Kamiokande detector[50] consisted of eleven events of energy 7.5 to 36 MeV, arriving within 12 s of each other. The signal detected by the IMB detector[51] consisted of eight events arriving within 6 seconds with an energy of 20 to 40 MeV. The neutrinos were detected in both detectors through neutrino-electron scattering. Electron neutrinos could also be detected via the reaction $\overline{\nu}_e p \rightarrow n e^+$. It is believed that most of the events observed were due to $\overline{\nu}_e$ interactions because $\sigma(\overline{\nu}_e p \rightarrow n e^+)$ is much larger than other neutrino cross sections at low energies.

Using the length of the neutrino pulse observed by the Kamiokande detector, an estimate on the upper limit of the neutrino mass can be calculated using the equation for Δt. This gives $m_\nu < 42$ eV, with $\Delta t = 12$ s, $E \approx 21.7$ MeV (where E is the median of the energy distribution) and $d = 50$ kpc. More sophisticated calculations have also been performed to calculate limits on m_ν. These calculations study the individual events, neutrino interactions in the earth's atmosphere and neutrino interactions in the core of the supernova that could cause it to cool faster than observed. Using data from both the IMB and Kamiokande detectors, Mayle *et. al.*[52] calculated an upper limit for m_ν, applicable to all three neutrino species, of 3 keV. A summary of the astrophysical and cosmological tau neutrino mass limits is shown in Figure 16.

3.3. Cosmological Limits

Limits on the mass of the three neutrino species can be calculated using properties of the standard model of cosmology which states that the universe is expanding from a state of extremely high temperatures. This expansion of the universe began with the big bang, $\sim 1.5 \times 10^{10}$ y ago, and continues today. Two elements of the standard model of cosmology are studied in this review: the energy density of the universe and nucleosynthesis.[4,54]

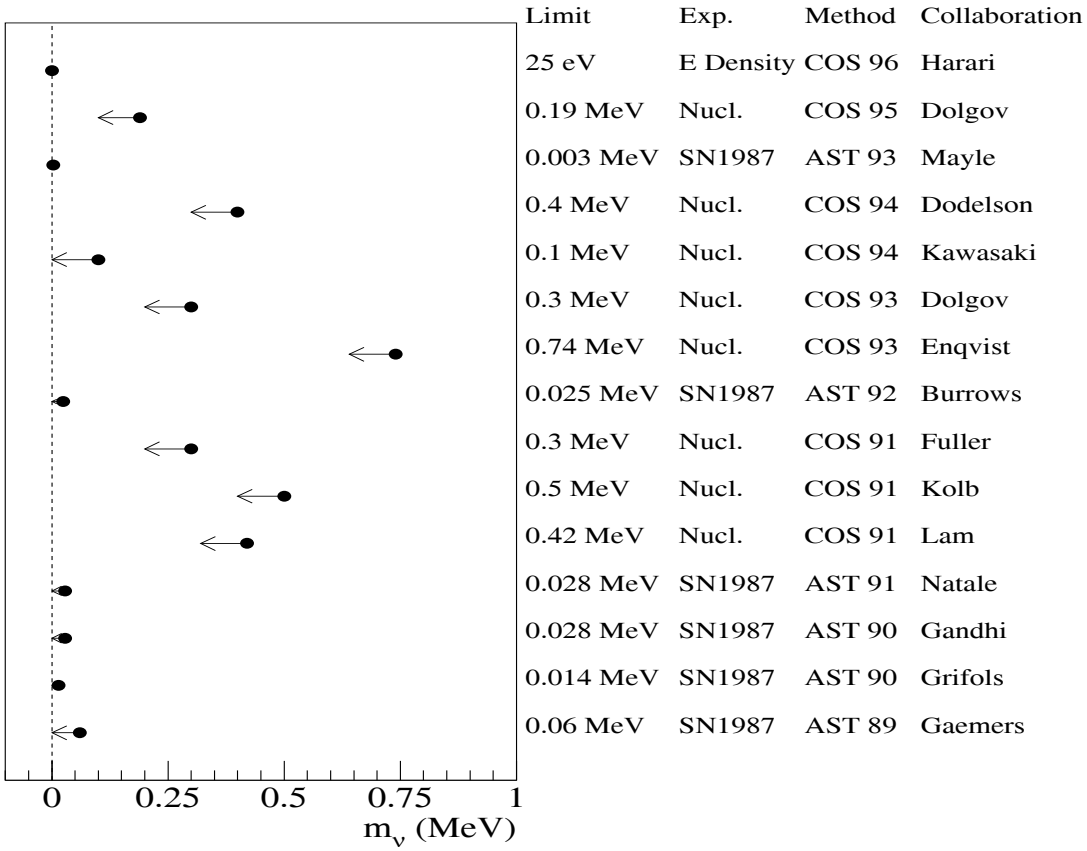

Figure 16: Summary of published astrophysical (AST) and cosmological (COS) tau neutrino mass limits.[4,6] The astrophysical limits are calculated from the SN1987A supernova explosion while the cosmological limits are calculated from the energy density of the universe and nucleosynthesis.

3.3.1. Energy Density of the Universe

A limit on the mass of the stable and unstable neutrinos can be made by requiring that the energy density of the three neutrino species, ρ_ν, must not exceed the energy density of the universe, ρ. The energy density can be expressed in units of the critical density, ρ_c, as

$$\rho = \Omega \rho_c, \tag{14}$$

where Ω is a constant whose value is not well known, but estimates suggest that at most Ω equals two.[4,17] If the critical density equals the true density of the universe, *i.e.* $\Omega = 1$, then the universe is flat. This implies that although the universe is expanding now it will ultimately after some time come to rest. The critical density for a homogeneous universe

has been calculated to be[4]

$$\rho_c = 1.1 \times 10^4 \, h^2 \ \frac{\text{eV}}{\text{cm}^3}, \tag{15}$$

where h is the Hubble's constant in units of 100 km s^{-1} Mpc^{-1}. The value of h is uncertain, but is estimated to be between 0.5–1.0.[17]

(i) Stable Neutrinos

If the neutrinos are stable and non-relativistic, then their energy density can be written as

$$\rho_\nu = \sum_{i=1}^{3} m_{\nu_i} n_{\nu_i}, \tag{16}$$

where m_{ν_i} is the mass of each neutrino species and n_{ν_i} is their respective number density. Limits on the neutrino masses can be calculated by requiring that the neutrino energy density must be less then the energy density of the universe, *i.e.* $\rho_\nu \leq \rho$.

The neutrino number density is predicted to have two values depending on whether the neutrinos are light (a few eV) or heavy (a few GeV).[4] During the early epochs of the universe, pions and nucleons were in equilibrium with the neutrinos, charged leptons and photons. Light neutrinos remained in equilibrium with the other particles as long as the temperature of the universe remained above 1 MeV. Thus during the early universe, from Bose-Einstein and Fermi-Dirac statistics,[4]

$$\frac{n_{\nu_i}}{n_\gamma} = \frac{3}{4}. \tag{17}$$

But as the universe aged, this relationship changed because the number of photons increased due to electron-positron annihilations, therefore[4]

$$\frac{n_{\nu_i}}{n_\gamma} = \frac{3}{11}. \tag{18}$$

Heavy neutrinos, on-the-other-hand, remain in equilibrium until the temperature of the universe reaches $kT \sim m_\nu/20$, approximately of order of a GeV. Thus the ratio of the heavy neutrino number density to the photon number density is predicted to be[17]

$$\frac{n_{\nu_i}}{n_\gamma} \sim 10^{-7} \left(\frac{m_{\nu_i}}{\text{GeV}} \right)^{-3}. \tag{19}$$

The photon number density is measured from blackbody radiation to be $n_\gamma \sim 400$ photons per cm^3.[17] Consequently, for light neutrinos $n_{\nu_i} \sim 110$ particles per cm^3, while for heavy neutrinos $n_{\nu_i} \sim 4 \times 10^{-5} (m_{\nu_i}/\text{GeV})^{-3}$ particles per cm^3.

If the neutrino energy density is required to be less than the energy density of the universe, then the mass of the light and heavy neutrinos are

$$\begin{aligned} \textstyle\sum_{i=1}^{3} m_{\nu_i} &\leq 100\Omega h^2 \text{ eV} \\ \text{and} \quad m_{\nu_i} &\geq 1.7[\Omega h^2]^{-1/2} \text{ GeV}, \end{aligned} \tag{20}$$

respectively. Note that for heavy neutrinos, the limit is only valid for individual neutrino species due to the form of n_{ν_i} given in equation (19). Limits can be derived for m_{ν_i} for both matter and radiation dominated universes. A matter dominated universe requires that $\Omega = 2$ and $h = 0.57$.[4] Therefore for light neutrinos $\sum_{i=1}^{3} m_{\nu_i} \leq 65$ eV, and for heavy neutrinos $m_{\nu_i} \geq 2.1$ GeV. A radiation dominated universe requires that $\Omega = 1$ and $h = 0.5$.[4] Therefore for light neutrinos $\sum_{i=1}^{3} m_{\nu_i} \leq 25$ eV (see Figure 16), and for heavy neutrinos $m_{\nu_i} \geq 3.4$ GeV. Consequently the energy density of the universe gives two allowed regions for stable neutrinos, light neutrinos below a few tens of eV and heavy neutrinos above the GeV range.

(ii) Unstable Neutrinos

For unstable neutrinos, the energy density of the decay products, ρ_{DP}, must be less than the current energy density of the universe. If a neutrino is heavy, of order GeV, then one has a matter dominated universe. However, the heavy neutrino's decay products, that are relativistic after the decay, then become dominant and cause the universe to be radiation dominated. Thus, assuming that the universe is currently radiation dominated by the decay products

$$\rho_{DP} = \rho_{\nu_i} \times \frac{T_{DecayTime}}{T_{Now}}, \tag{21}$$

where ρ_{ν_i} is the density of the parent neutrino had it not decayed, $T_{DecayTime}$ is the time that the decay took place and T_{Now} is the present time. Thus $\rho_{DP} \leq \rho$ leads to an upper bound on the mass (or lifetime) of any neutrino species. For a radiation dominated universe, the limits are[4]

$$\begin{aligned} m_{\nu_i}^2 \tau_{\nu_i} &\leq 2 \times 10^{20} \text{ eV}^2\text{s} \quad \text{for } m_{\nu_i} \leq \text{a few MeV} \\ \text{and} \quad \tfrac{\tau_{\nu_i}}{m_{\nu_i}^4} &\leq 1.5 \times 10^{-22} \text{ eV}^{-4}\text{s} \quad \text{for } m_{\nu_i} > \text{a few MeV}. \end{aligned} \tag{22}$$

Consequently, if the decay time of any neutrino is known then an upper mass bound for an unstable neutrino can be calculated or *vice versa*.

3.3.2. Nucleosynthesis

The synthesis of light elements (^{2}H, ^{3,4}He, ^{7}Li) can be used to set a limit on m_{ν_τ}, since the mass ratio of helium to hydrogen (number of neutrons to protons) depends on the number of neutrino flavours.[17] Immediately after the Big Bang created the universe, the universe began to cool. At a temperature of approximately 10^{11} K, the remnant baryons are in thermal equilibrium through the weak reactions[17]

$$\begin{aligned} & n + e^+ \leftrightarrow p + \overline{\nu}_e \\ \text{and} \quad & n + \nu_e \leftrightarrow p + e^-. \end{aligned}$$

No complex nuclei were formed as the temperature was too high. However, below 10^{11} K the neutron production cross-section is smaller than the proton production cross-section. Therefore the number of neutrons to protons decreased. In addition, the neutrino cross-sections fall along with the density and at $T = 10^{10}$ K are decoupled from the remaining matter.[16] The age of the universe is now one second.

Later, around 225 seconds ($T = 10^9$ K) after the Big Bang, primordial nucleosynthesis begins with[17]

$$n + p \rightarrow d + \gamma,$$

and the subsequent formation of ^{4}He and small amounts of ^{3}He and ^{7}Li. This sequence is possible because the time is short enough that neutrons have not disappeared from beta-decay and that the temperature is low enough that the deuterons do not photodisintegrate. About 10^6 years later the temperature of the universe has fallen enough (to about 2000 K) to allow the combination of electrons and nuclei into neutral atoms.

If the expansion rate of the universe increases, then the weak interactions that determine the ratio of neutrons to protons stops earlier, thus causing an overproduction of the light element ^{4}He. The observable upper bound on the ^{4}He abundance provides an upper bound on the total energy density at the moment of nucleosynthesis; this can be expressed as the number of neutrino families, $N_\nu = 3 \pm \delta N_\nu$, where $\delta N_\nu = 0.3$.[55] δN_ν is calculated from the abundance of light elements and is known as the effective number of relativistic neutrinos; it can be used to measure bounds on the neutrino mass. Dolgov *et. al.* used the above technique and estimated an upper bound on the tau neutrino mass of 190 keV (see Figure 16).[56]

4. Discussion and Consequences of a Massive Tau Neutrino

A massive ν_τ has several consequences to the fields of particle physics and cosmology. Tau neutrinos can have generation mixing, consequently, neutrinos may oscillate from one type to another. The ν_τ may have a lifetime and magnetic moment. Tau neutrinos are also candidates for the dark or missing mass component of the universe. These topics will be discussed and limits of the ν_τ lifetime and magnetic moment will be presented in this section.

4.1. Neutrino mixing and oscillations

In 1957, Pontecorvo[57] suggested that if lepton number was not conserved and if the neutrino species were massive particles, then neutrinos could oscillate from one flavour to another. This concept, known as *neutrino mixing*, occurs because the observed mass of the neutrino flavour ν_l $(l = e, \mu, \tau)$ may be a superposition of the unmixed weak eigenstates ν_i' $(i = 1, 2, 3)$ each with a different mass m_{ν_i}, such that[17]

$$\nu_l = \sum_{i=1}^{3} U_{li} \nu_i' \tag{23}$$

where U_{li} is a three-dimensional unitary mixing matrix.

The theory of neutrino mixing can be simplified by considering only two neutrino flavours where there are only two parameters:[58] the mixing angle, θ, and the square of the mass difference between the two neutrinos, δm^2. The two physical neutrinos, say ν_μ and ν_τ, will be a linear combination of the unmixed weak eigenstates ν_2' and ν_3' as given by a two-dimensional unitary transformation, involving the mixing angle θ,[17]

$$\begin{aligned} \nu_\tau &= \nu_2' \cos\theta + \nu_3' \sin\theta \\ \nu_\mu &= -\nu_2' \sin\theta + \nu_3' \cos\theta. \end{aligned} \tag{24}$$

As a pure neutrino beam propagates in time, say from $t = 0$, one may observe a change in the quantity of a specific neutrino flavour contained within the beam. This observation allows one to measure the probability of observing neutrino oscillations. For example, for a muon beam, the probability of observing a ν_τ or a ν_μ is expressed, respectively as[17]

$$\begin{aligned} P(\nu_\mu \to \nu_\tau) &= \sin^2 2\theta \sin^2 \Delta \\ P(\nu_\mu \to \nu_\mu) &= 1 - \sin^2 2\theta \sin^2 \Delta, \end{aligned} \tag{25}$$

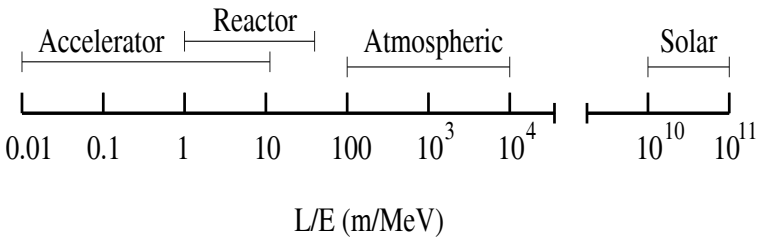

Figure 17: Illustration of regions of L/E that are accessible in various experiments.

where $\Delta = 1.27 \times \delta m^2 \times L/E$. The constant 1.27 applies if δm is expressed in eV, while L, the distance from the source, is expressed in metres and E the beam energy in MeV. From the probabilities it can be observed that the intensities oscillate as a function of distance. There are two methods used to search for neutrino oscillations. In experiments referred to as *appearance* experiments, one starts with the ν_l beam and looks for neutrinos $\nu_{l'}$ with a *different* flavour at a distance L from the neutrino source. If oscillations are present then $P(\nu_l \rightarrow \nu_{l'})$ is non-vanishing. In *disappearance* experiments, the neutrino beam which started as a ν_l beam, is intercepted by a detector sensitive to the *same* neutrino flavour at varying distances L. If oscillations are present, the probability $P(\nu_l \rightarrow \nu_l)$ is smaller than unity.

To gain a perspective of the range of sensitivity to L/E for various oscillation experiments see Figure 17. This plot shows several regions of interest for neutrino physics. At large L/E, neutrinos come from extraterrestrial sources such as the sun, where the neutrinos must travel large distances to get to the earth. If L/E is between 100 and 10,000, then the neutrinos originate from atmospheric weak interactions in the earth's atmosphere. Finally, if the ratio is less then 10, then the neutrinos are created at high energies in reactors and accelerators, these neutrinos have a very high energy and thus only have to travel a short distance before oscillations take place.

No measurement has unambiguously observed neutrino oscillations. However, if neutrino oscillations are observed, then neutrinos are massive since experiments measure the quantity δm^2. The results of oscillation experiments are usually presented in the form of *exclusion plots* exhibiting the allowed and forbidden regions in the $(\sin^2 2\theta, \delta m^2)$ parameter space. Figure 18 shows current limits on δm^2 and $\sin^2 2\theta$ from five accelerator experiments.[59] For example, a limit of $\delta m^2 < 0.2$ eV^2 is obtained for full mixing at $\sin^2 2\theta = 1$.

If neutrino oscillations are observed, then the solar neutrino problem may have a solution. The solar neutrino problem describes the difference between the observed neutrino flux and the theoretical expected flux as observed on the surface of the earth. The theo-

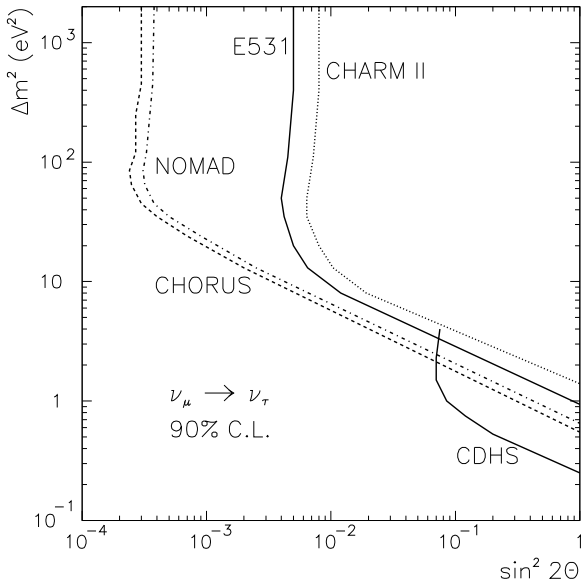

Figure 18: Limits on neutrino oscillations $\nu_\mu \rightarrow \nu_\tau$. The difference of mass squared of the mass eigenstates is plotted against $\sin^2 2\theta$, where θ is the mixing angle. The five limits presented are from accelerator experiments. The regions to the right of the curves are excluded at the 90% confidence level.

retically predicted flux calculated for the CNO cycle of the sun is approximately 8 SNU,[60] where 1 SNU is defined to be 10^{-36} events/sec target atom. Experiments performed by the Kamiokande[61] and Davis[60] collaborations have used neutrino capture to observe the electron neutrinos emitted by the sun, for example, Davis uses the reaction ν_e ^{37}Cl $\rightarrow$ e^- ^{37}Ar.[60] The results of these capture experiments have yielded a flux of only $\sim$ 2 SNU.[60,61] The theory of neutrino mixing allows electron neutrinos to change to either undetectable muon or tau neutrinos, thus causing the observed electron neutrino flux to be less than the predicted value.

4.2. The ν_τ Lifetime

If lepton number is not conserved, then a massive tau neutrino may be unstable. In this case, there are three decays of the tau neutrino that may occur. The first is the $\nu_\tau \rightarrow \nu_x \overline{\nu}_x \nu_y$ decay, where ν_x and ν_y are not ν_τ (see Figure 19), however, the decay products would be difficult to observe. The second and third decays of the tau neutrino, $\nu_\tau \rightarrow \nu_x \gamma$ (see Figure 20) and $\nu_\tau \rightarrow e^+ e^- \nu_x$ (see Figure 21), include particles that are more easily identified using available calorimeters.

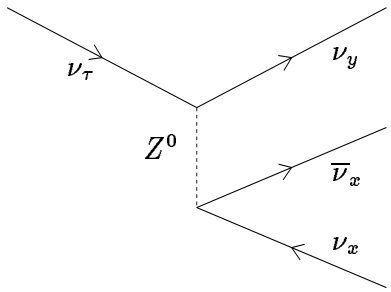

Figure 19: Feynman diagram for the decay $\nu_\tau \rightarrow \nu_x \overline{\nu}_x \nu_y$.

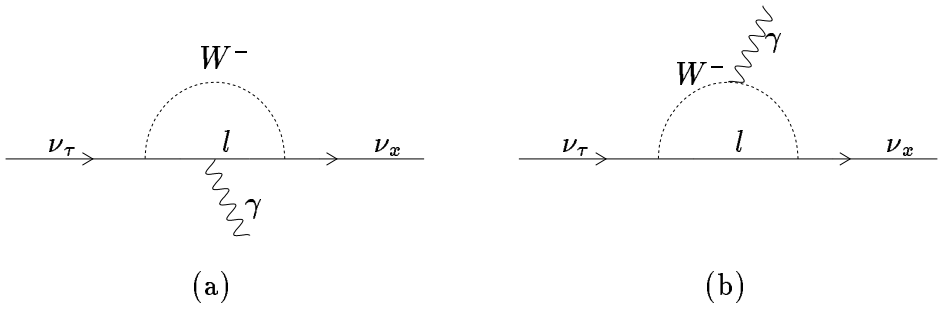

Figure 20: Feynman diagrams for the decay $\nu_\tau \rightarrow \nu_x \gamma$.

Predictions for the width of the $\nu_\tau \rightarrow \nu_x \gamma$ decay have been discussed by several physicists.[17,62] Although no such decays have been observed, their non-observation can permit one to set a limit on the decay rate of the massive neutrino. Current experimental information gives a $\nu_\tau \rightarrow \nu_x \gamma$ decay rate of[17]

$$\Gamma \equiv \frac{1}{T_{\nu_\tau}} \approx \left[\frac{m_{\nu_\tau}}{30\text{eV}}\right]^5 10^{-29}\text{y}^{-1} \tag{26}$$

assuming that $m_{\nu_\tau} \gg m_{\nu_x}$.

Limits on T_{ν_τ} can also be measured using astrophysical and cosmological properties. One interesting limit on T_{ν_τ} has been derived from observations of the supernova explosion SN1987A. As previously stated, a massive star can collapse to form a neutron star emitting a massive number of neutrinos. If some of these neutrinos are massive and unstable, then the decay of neutrinos of that species will produce copious numbers of photons. This fact can be exploited to place a constraint on the $\nu_\tau \rightarrow \nu_x \gamma$ decay modes of the massive neutrino species. The first limit performed by Cowsik[63] calculated the integrated flux of photons resulting from the decay of neutrinos produced by all supernova explosions throughout the history of the universe. Cowsik then insisted that this flux be less than the measured photon background flux at energies of order 10 MeV. The limit $T_{\nu_\tau}/m_{\nu_\tau} \geq 3 \times 10^{16}$s/eV was

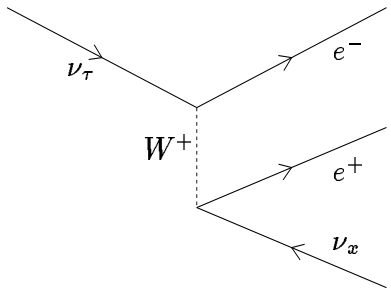

Figure 21: Feynman diagram for the decay $\nu_\tau \rightarrow e^+e^-\nu_x$.

obtained, assuming that the branching ratio of the massive neutrino to all radiative modes is unity. Newer limits have since been performed that have put much stricter limits on T_{ν_τ}. For example, Kolb & Turner[64] have obtained $T_{\nu_\tau} \geq 8.4 \times 10^{17}/m_{\nu_\tau}$s eV. Substituting the ALEPH limit on m_{ν_τ} into the above neutrino lifetime predictions, it can be shown that T_{ν_τ} is at least 2.5×10^7s.

4.3. Magnetic Moment

Dirac and Majorana neutrinos can be distinguished by measuring their electromagnetic properties. Dirac neutrinos can have a nonvanishing magnetic dipole moment, and perhaps even an electric dipole moment. Majorana neutrinos, on the other hand, must have vanishing dipole moments because CPT invariance must hold when a particle is identical to its antiparticle. The standard model predicts the magnetic moment of a Dirac neutrino of mass m_{ν_τ} to be[65]

$$\mu_{\nu_\tau} = \frac{3eG_F}{8\pi^2\sqrt{2}} m_{\nu_\tau} \approx 3 \times 10^{-19} \frac{m_{\nu_\tau}}{1\text{eV}} \mu_{Bohr}, \tag{27}$$

where μ_{Bohr} is the Bohr magneton. Using the measurement of m_{ν_τ} from ALEPH, the magnetic moment of Dirac neutrinos is calculated to be less than $7.5 \times 10^{-12}\mu_{Bohr}$. Note that this value is currently too small to be measured by existing experiments, even for a relatively large tau neutrino mass.

A limit on the ν_τ magnetic moment can also be estimated from single photon searches, such as the process $e^+e^- \rightarrow \nu\overline{\nu}\gamma$ (see Figure 22).[66,67] At energies below the Z^0 resonance the dominant contribution to the process $e^+e^- \rightarrow \nu\overline{\nu}\gamma$ involves the exchange of a virtual photon (see Figure 22(a)). Dependence on the magnetic moment comes from a direct coupling to the virtual photon at the $\nu\overline{\nu}\gamma$ vertex. The observed photon is a result of initial state bremsstrahlung. Note that final state radiation at low energies might take place, but its effect on μ_{ν_τ} would be small. Searches by the ASP[68] collaboration at SLAC for $e^+e^- \rightarrow \nu\overline{\nu}\gamma$ events have been performed by requiring that the energy of the photon be less than

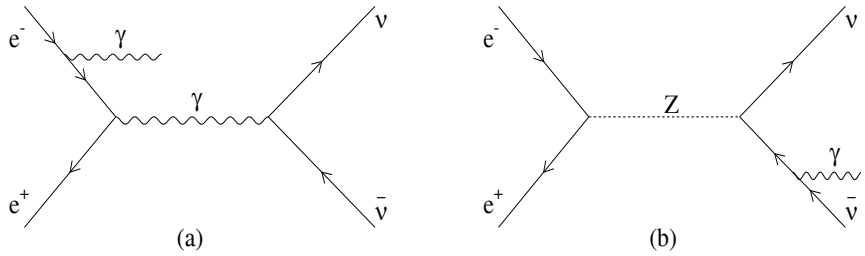

Figure 22: Examples of Feynman diagrams for the reaction $e^+e^- \to \nu\overline{\nu}\gamma$.

10 GeV, and that the polar angle be less than 20°. After applying these requirements the ASP[68] collaboration reported that the magnetic moment is at most $8 \times 10^{-6}\mu_{Bohr}$ at a 90% confidence level. Note that this limit only holds under the assumption that the magnetic moment coupling remains point-like at the centre-of-mass energy.[66]

At LEP energies (E_{CM} = 91 GeV) the $e^+e^- \to \nu\overline{\nu}\gamma$ reaction involves the exchange of the Z^0. Therefore dependence on the magnetic moment comes from the photon being emitted from one of the outgoing neutrinos, also known as final state radiation (see Figure 22(b)). Searches at LEP for $e^+e^- \to \nu\overline{\nu}\gamma$ events have been performed by requiring that the energy of the photon be greater than 10 GeV, and that the polar angle of the direction of missing momentum be greater than $\sim$26° with respect to the beam axis.[22] These requirements ensure that the photon does not originate from initial state bremsstrahlung. After applying these requirements the LEP experiments did not observe any $e^+e^- \to \nu\overline{\nu}\gamma$ events, thus implying that $\mu_{\nu_\tau} \leq 5.5 \times 10^{-6}\mu_{Bohr}$ at a 90% confidence level.[67]

Estimates of the magnetic moment have also been calculated using nucleosynthesis, cosmic electromagnetic background and from red giant luminosity. The different estimates of the Dirac ν_τ magnetic moment have a range of $\mathcal{O}(\propto\prime^{-}\!\!)\mu_{\mathcal{B}l\langle\nabla}$ to $\mathcal{O}(\propto\prime^{-\infty\in})\mu_{\mathcal{B}l\langle\nabla}$.

4.4. Dark Matter

The expansion of the universe will stop if it contains sufficient mass for gravity to provide an adequate attractive force to slow down and reverse the expansion. The critical density of the universe required to stop this expansion is 1.1×10^4 eV/cm^3. Currently it has been observed that the average density of the baryons present in the universe is approximately 2.8×10^3 eV/cm^3 and thus on its own is not large enough to reach critical density and reverse the expansion of the universe.[69] It is known that the dynamics of galaxies and clusters indicates that there is matter present which is not luminous and which may

bring the average density to near critical. This extra matter is called *dark* or *missing* matter. It may be present in the form of undeveloped stars or cold compact stellar objects. It could also be present in the form of unknown neutral particles with mass, or massive neutrinos.

The present number density of neutrinos of all types (including antineutrinos) in the universe is estimated[17] to be 110 cm^{-3}. Thus if all three neutrino species have an average mass of approximately 33 eV, the neutrino density, ρ_ν, would be enough for the universe to reach the critical density. If not enough dark matter is found, the universe will expand forever. If the critical density is exceeded, the expansion will slow down, stop and reverse, resulting in the reverse of the big bang, the *big crunch*, thus ending the universe in its present state.

5. Conclusion

In 1932, Pauli postulated the existence of the electron neutrino to explain the observation of the continuous electron energy spectrum of beta-decays. Two more neutrinos, ν_μ and ν_τ, were hypothesised to exist in the Standard Model, however, only ν_e and ν_μ have been directly observed by experiment. There is no clear evidence that neutrinos have mass, however, if they do have mass then there are several important consequences to the fields of particle physics, cosmology and astrophysics.

The mass of the neutrinos has not been directly measured. However, limits on the mass of the neutrinos are inferred from various experiments and theoretical models. The best limit on m_{ν_e} was measured from the end-point of tritium decays giving $m_{\nu_e} < 5.1$ eV.[6] The best limit on m_{ν_μ} was measured from $\pi^+ \rightarrow \mu^+\nu_\mu$ decays giving $m_{\nu_\mu} < 160$ keV.[11] Finally, the best limit on m_{ν_τ} was measured from $\tau^- \rightarrow 3\pi^- 2\pi^+(\pi^0)\nu_\tau$ decays giving $m_{\nu_\tau} < 24$ MeV.[20]

Several model dependent studies were used to set a limit on m_{ν_τ}. A comparison of the $\tau^- \rightarrow e^-\bar{\nu}_e\nu_\tau$ decay width with the Standard Model prediction gave $m_{\nu_\tau} < 71$ MeV.[49] The supernova explosion, SN1987A, gave $m_{\nu_\tau} < 3$ keV.[52] Requiring that the neutrino energy density be less then energy density of the universe gave a limit for stable neutrinos of $\sum_{i=1}^{3} m_{\nu_i} \leq 25$ eV, for light neutrinos, and $m_{\nu_i} \geq 3.4$ GeV, for heavy neutrinos.[4] Limits can also be obtained for unstable neutrinos which depend on the lifetime of the neutrino. Finally, primordial nucleosynthesis gave an upper limit on m_{ν_τ} of 190 keV.[56]

If neutrinos are massive, then there are several consequences. If lepton number is not conserved, then neutrinos may mix and subsequently oscillate from one type to another. Unstable neutrinos would have a lifetime and estimates suggest that T_{ν_τ} is at least 2.5×10^7 s.

Dirac neutrinos would have a non-vanishing magnetic moment in the range $\mathcal{O}(\propto\prime^{-})\mu_{\mathcal{B}l\langle\nabla}$ to $\mathcal{O}(\propto\prime^{-\infty\in})\mu_{\mathcal{B}l\langle\nabla}$. The solar neutrino problem may have a solution as a result of neutrino mixing. Finally, the dark matter problem could be solved if neutrinos have an average mass of only 33 eV.

Further explorations of the properties of the tau neutrino are currently being conducted by several experiments. The LEP collaborations are currently exploring new methods and different tau decays to reduce the limit on m_{ν_τ}. The study of neutrino oscillations of the type $\nu_\mu \longleftrightarrow \nu_\tau$ is being conducted by the NOMAD and CHORUS collaborations at CERN. A proposed experiment at Fermilab (P803) will also explore $\nu_\mu \longleftrightarrow \nu_\tau$ oscillations, but with an increased sensitivity to ν_τ, due to a longer beam path. New experiments are also being conducted to solve the solar neutrino problem. The Sudbury Neutrino Observatory (SNO) and Kamiokande II experiments hope to measure the solar neutrino flux of all three neutrino flavours and thus be able to account for the discrepancy between the theoretical and experimental flux measurements. With technology giving rise to new experiments, one should be able to observe the tau neutrino in the near future and hopefully receive a definitive answer as to whether or not neutrinos have mass.

References

1. W. Pauli, *Diracs Wellengleichung des Elektrons und geomtrische Optic*, Helv. Phys. Act. **5** (1932) 179;
   C.P. Enz, *50 Years Ago Pauli Invented The Neutrino*, Helv. Phys. Act. **54** (1981) 411.
2. F. Reines and C.L. Cowan, Jr., Phys. Rev. **92** (1953) 830.
3. G. Danby *et. al.*, Phys. Rev. Lett. **9** (1962) 36.
4. H. Harari *et. al.*, Nucl. Phys. **B 292** (1987) 251.
5. A.J. Weinstein and R. Stroynowski, Ann. Rev. Nucl. Part. Sci. **43** (1993) 457.
6. *Review of Particle Properties* Phys. Rev. **D 50** (1994).
7. D.H. Perkins, *Introduction to High Energy Physics. Third Ed.*, Addison Welsley, 1987.
8. K.E. Bergkvist, Nucli. Phys. **B339** (1972) 319.
9. E.F. Tretyakov *et. al.*, Proc. Neutrino Conf. Aachen, 1976.
10. W.H. Barkas, W. Branbaum and F.M. Smith, Phys. Rev. **101** (1956) 778.
11. K. Assamagan *et. al.*, Phys. Lett. **B 335** (1994) 231.
12. R.G. Robertson and D.A. Knapp, Ann. Rev. Nucl. Part. Sci. **38** (1988) 185.
13. ALEPH Collaboration, D. Buskulic *et. al.* Phys. Lett. **B 349** (1995) 585.
14. F. Halzen and A. Martin, *Quarks and Leptons*, Wiley, 1984;
    H. Frauenfelder and E. Henley, *Subatomic Physics, Second Ed.*, Prentice Hall, Englewood Cliffs, N.J., U.S.A.,1991.
15. S.L. Glashow, J. Hiopoulos and L. Maiani, Phys. Rev. **D 2** (1970) 1285;
    S. Weinberg, Phys. Rev. Lett. **19** (1967) 1264;
    A. Salam, *Elementary Particle Theory* Ed. N. Svartholm, (Almquist and Wilsells, Stockholm, 1969) 357.
16. G. Gelmini and E. Roulet, Rept. Prog. Phys. **58** (1995), 1207.
17. F. Beohm and P. Vogel, *Physics of Massive Neutrinos*, Cambridge University Press (1987).
18. Perl, *et al.*, *Properties of Anomalous $e\mu$ Events Produced in e^-e^+ Annihilation*, Phys. Lett., **B 63** (1976) 466;
    Feldman, *et al.*, *Inclusive Anomalous Muon Production in e^-e^+ Annihilation*, Phys. Rev. Lett., **B 38** (1977) 117 and 576.
19. OPAL Collaboration, G. Alexander *et. al.*, CERN-PPE/96-042.
20. ALEPH Collaboration, D. Buskulic, *et. al.*, CERN-PPE/95-03.
21. DELPHI Collaboration, P. Abreu, *et. al.*, CERN-PPE/95-114.
22. L3 Collaboration, O. Adriani, *et. al.*, Phys. Rep. **236** (1993) 1.
23. S. Abachi *et. al.*, Phys. Rev. **D 35** (1987) 2880.
24. ARGUS Collaboration, H. Albrecht *et. al.*, Phys. Lett. **B 291** (1992) 221.
25. CLEO II Collaboration, D. Cinnabro *et. al.*, Phys. Rev. Lett. **70** (1993) 3700.
26. BES Collaboration, J.Z. Bai *et. al.*, SLAC Preprint SLAC-PUB-6930.
27. C.A. Blocker *et. al.*, Phys. Lett. **B 109** (1982) 119.
28. W. Bacino *et. al.*, Phys. Rev. Lett. **42** (1979) 749.
29. ALEPH Collaboration, D. Decamp *et. al.*, Nucl. Inst. Meth. **A 294** (1990) 121.
30. ALEPH Collaboration, D. Decamp *et. al.*, Z. Phys. **C 54** (1992) 211.
31. J.J. Gomez-Cadenas and C.M. Gonzalez-Garcia, Phys. Rev. **D 39** (1989) 1370.

32. OPAL collaboration, Z. Phys. **C 65** (1995) 183.
33. ARGUS Collaboration, H. Albrecht *et. al.*, Phys. Lett. **B 207** (1988) 149.
34. CLEO Collaboration, Phys. Rev. **D 35** (1987) 2747.
35. S. Abachi *et. al.*, Phys. Rev. Lett. **56** (1986) 1039.
36. ARGUS Collaboration, H. Albrecht *et. al.*, Phys. Lett. **B 163** (1985) 404.
37. MARK II collaboration, Phys. Rev. Lett. **54** (1985) 2489.
38. MARK II collaboration, Phys. Rev. **D 32** (1985) 800.
39. DELCO collaboration, Phys. Rev. Lett. **54** (1985) 624.
40. ALEPH Collaboration, D. Buskulic *et. al.*, Z. Phys. **C 62** (1994) 539.
41. Y.S. Tsai, Phys. Rev. **D4** (1971) 2821.
42. W.J. Marciano and A. Sirlin, Phys. Rev. Lett. **61** (1988) 1815.
43. OPAL Collaboration, G. Alexander *et. al.*, CERN-PPE/95-142.
44. ALEPH Collaboration, D. Buskulic *et. al.*, CERN-PPE/95-127.
45. DELPHI Collaboration, P. Abreu *et. al.*, CERN-PPE/95-114.
46. OPAL Collaboration, presented at the International Lepton-Photon Conference, Beijing, China, 1995;
    ALEPH Collaboration, D. Buskulic *et. al.*, CERN-PPE/95-128;
    DELPHI Collaboration, P. Abreu *et. al.*, CERN-PPE/95-154;
    L3 Collaboration, presented at the Third Workshop on Tau Lepton Physics, Montreux, Switzerland, 1994.
47. CLEO Collaboration, M. Battle *et. al.*, Phys. Lett. **B 291** (1992) 488.
48. SLD Collaboration, K. Abe *et. al.*, SLAC-PUB-95-6767.
49. R.J. Sobie, R.K. Keeler and I. Lawson, *An upper limit on the tau neutrino mass from leptonic tau decays*, Z. Phys. **C 70** (1996) 383.
50. K.S. Hirata *et. al.*, Phys. Rev. Lett. **58** (1987) 1490.
51. R.M. Bionta *et. al.*, Phys. Rev. Lett. **58** (1987) 1494.
52. R. Mayle *et. al.*, Phys. Lett. **F 317** (1993) 119.
53. S. Weinberg, *Gravitation and Cosmology*, Wiley, 1972.
54. G. Gelmini, *Neutrino Physics*, Proceedings of an International Workshop Held in Heidelberg (1987) 44.
55. T.P. Walker *et. al.*, J. Astrophys. **376** (1991) 51.
56. A.D. Dolgov, K. Kainulainen and I.Z. Rothstein, Phys. Rev. **D 51** (1995) 4129.
57. B. Pontecorvo, Zh. Eksp. Teor. Fiz. **33** (1957) 549; *ibid* **34** (1958) 247.
58. X. Shi, D.N. Schramm and J.N. bahcall, Phys. Rev. Lett. **69** (1992) 717.
59. Nomad Collaboration, Marco Laveder *et. al.*, *The NOMAD Experiment at the CERN SPS: A Status Report*, Presented at TAUP95 (Toledo, Spain, September 1995) and Submitted to Nucl. Phys. B (Proc. Suppl) (1995).
60. R. Davis Jr., A.K. Mann and L. Wolfenstein, Ann. Rev. Nucl. Part. Sci. **39** (1989) 467.
61. K.S. Hirata *et. al.*, Phys. Rev. Lett. **63** (1989) 16.
62. M. Roos, *Neutrino Physics*, Proceedings of an International Workshop Held in Heidelberg (1987) 57.
63. R. Cowsik, Phys. Rev. Lett. **39** (1977) 784.
64. E. Kolb and M. Turner, Phys. Rev. Lett. **62** (1989) 509.
65. W.J. Marciano and A.I. Sanda Phys, Lett. **B 67** (1977) 303;
    B.W. Lee and R.E. Shrock, Phys. Rev. **D 16** (1977) 1444.
66. G.F. Giudice, Phys. Lett. **B 251** (1990) 460.

67. T.M. Gould and I.Z. Rothstein, Phys. Lett. **B 333** (1994) 545.
68. ASP Collaboration, C. Hearty *et. al.*, Phys. Rev. **D 39** (1989) 3207.
69. M.S.C. Williams, *Nuclear and Particle Physics*, Oxford University Press (1992).